



TITLE:

Search for bottom squark pair production in
proton–proton collisions at $\sqrt{s} = 13$ TeV
with the ATLAS detector

AUTHOR(S):

ATLAS Collaboration; Kunigo, T.; Monden, R.;
Sumida, T.; Takashima, R.; Tashiro, T.

CITATION:

ATLAS Collaboration ...[et al]. Search for bottom squark pair production in proton–proton collisions at $\sqrt{s} = 13$ TeV with the ATLAS detector. The European Physical Journal C 2016, 76(10): 547.

ISSUE DATE:

2016-10

URL:

<http://hdl.handle.net/2433/251072>

RIGHT:

© CERN for the benefit of the ATLAS collaboration 2016. This article is published with open access at Springerlink.com; This article is distributed under the terms of the Creative Commons Attribution 4.0 International License (<http://creativecommons.org/licenses/by/4.0/>), which permits unrestricted use, distribution, and reproduction in any medium, provided you give appropriate credit to the original author(s) and the source, provide a link to the Creative Commons license, and indicate if changes were made.



Search for bottom squark pair production in proton–proton collisions at $\sqrt{s} = 13$ TeV with the ATLAS detector

ATLAS Collaboration*

CERN, 1211 Geneva 23, Switzerland

Received: 29 June 2016 / Accepted: 16 September 2016 / Published online: 6 October 2016

© CERN for the benefit of the ATLAS collaboration 2016. This article is published with open access at Springerlink.com

Abstract The result of a search for pair production of the supersymmetric partner of the Standard Model bottom quark (\tilde{b}_1) is reported. The search uses 3.2 fb^{-1} of pp collisions at $\sqrt{s} = 13$ TeV collected by the ATLAS experiment at the Large Hadron Collider in 2015. Bottom squarks are searched for in events containing large missing transverse momentum and exactly two jets identified as originating from b -quarks. No excess above the expected Standard Model background yield is observed. Exclusion limits at 95 % confidence level on the mass of the bottom squark are derived in phenomenological supersymmetric R -parity-conserving models in which the \tilde{b}_1 is the lightest squark and is assumed to decay exclusively via $\tilde{b}_1 \rightarrow b\tilde{\chi}_1^0$, where $\tilde{\chi}_1^0$ is the lightest neutralino. The limits significantly extend previous results; bottom squark masses up to 800 (840) GeV are excluded for the $\tilde{\chi}_1^0$ mass below 360 (100) GeV whilst differences in mass above 100 GeV between the \tilde{b}_1 and the $\tilde{\chi}_1^0$ are excluded up to a \tilde{b}_1 mass of 500 GeV.

1 Introduction

Supersymmetry (SUSY) [1–6] provides an extension of the Standard Model (SM) that solves the hierarchy problem [7–10] by introducing supersymmetric partners of the known bosons and fermions. In the framework of the R -parity-conserving minimal supersymmetric extension of the SM (MSSM) [11–13], SUSY particles are produced in pairs and the lightest supersymmetric particle (LSP) is stable, providing a possible candidate for dark matter [14, 15]. In a large variety of models the LSP is the lightest neutralino ($\tilde{\chi}_1^0$). Naturalness considerations [16, 17] suggest that the supersymmetric partners of the third-generation SM quarks are the lightest coloured supersymmetric particles. This may lead to the lightest bottom squark (\tilde{b}_1) and top squark (\tilde{t}_1) mass

eigenstates¹ being significantly lighter than the other squarks and the gluinos. As a consequence, \tilde{b}_1 and \tilde{t}_1 could be pair-produced with relatively large cross-sections at the Large Hadron Collider (LHC).

This paper presents a search for the pair production of bottom squarks decaying exclusively as $\tilde{b}_1 \rightarrow b\tilde{\chi}_1^0$ using 3.2 fb^{-1} of proton–proton (pp) collisions at $\sqrt{s} = 13$ TeV collected by the ATLAS experiment at the LHC in 2015. A SUSY particle mass hierarchy with this exclusive decay has been predicted by various phenomenological MSSM models [18]. Searches with the $\sqrt{s} = 8$ TeV LHC Run-1 dataset at ATLAS and CMS have set limits on \tilde{b}_1 masses in such scenarios. For $\tilde{\chi}_1^0$ masses around 100 GeV, exclusion limits at 95 % confidence level (CL) up to 620 and 680 GeV have been reported by the ATLAS [19] and CMS [20] collaborations, respectively. The searches were performed in events characterized by the presence of large missing transverse momentum and two jets identified as containing b -hadrons (b -jets). In Run 2 of the LHC the production cross-section rises due to the increase of the centre-of-mass energy of the pp collisions. For instance, for a \tilde{b}_1 with a mass of 800 GeV, the production cross-section increases by almost a factor of ten going from $\sqrt{s} = 8$ TeV to $\sqrt{s} = 13$ TeV. In addition, the sensitivity of the analysis benefits from the improved algorithms adopted to identify b -jets and use of information from the newly installed pixel layer in the Run-2 ATLAS detector. The search strategy at 13 TeV closely follows the previous ATLAS studies, with signal regions defined to provide sensitivity to the kinematic topologies arising from different mass splittings between the bottom squark and the neutralino.

2 ATLAS detector

The ATLAS detector [21] is a multi-purpose particle physics detector with a forward-backward symmetric cylindrical

* e-mail: atlas.publications@cern.ch

¹ Scalar partners of the left-handed and right-handed chiral components of the bottom quark ($\tilde{b}_{L,R}$) or top quark ($\tilde{t}_{L,R}$) mix to form mass eigenstates for which \tilde{b}_1 and \tilde{t}_1 are defined as the lighter of the two.

geometry and nearly 4π coverage in solid angle.² The inner tracking detector consists of pixel and silicon microstrip detectors covering the pseudorapidity region $|\eta| < 2.5$, surrounded by a transition radiation tracker which enhances electron identification in the region $|\eta| < 2.0$. Between Run 1 and Run 2, a new inner pixel layer, the Insertable B-Layer (IBL) [22], was inserted at a mean sensor radius of 3.3 cm. The inner detector is surrounded by a thin superconducting solenoid providing an axial 2 T magnetic field and by a fine-granularity lead/liquid-argon (LAr) electromagnetic calorimeter covering $|\eta| < 3.2$. A steel/scintillator-tile calorimeter provides hadronic coverage in the central pseudorapidity range ($|\eta| < 1.7$). The endcap and forward regions ($1.5 < |\eta| < 4.9$) of the hadronic calorimeter are made of LAr active layers with either copper or tungsten as the absorber material. An extensive muon spectrometer with an air-core toroid magnet system surrounds the calorimeters. Three layers of high-precision tracking chambers provide coverage in the range $|\eta| < 2.7$, while dedicated fast chambers allow triggering in the region $|\eta| < 2.4$. The ATLAS trigger system consists of a hardware-based level-1 trigger followed by a software-based high-level trigger [23].

3 Data and simulated event samples

The data used in this analysis were collected by the ATLAS detector in pp collisions at the LHC with a centre-of-mass energy of 13 TeV and 25 ns proton bunch crossing interval during 2015. After applying beam-, data- and detector-quality criteria, the available dataset corresponds to an integrated luminosity of 3.2 fb^{-1} with an uncertainty of $\pm 5\%$. The uncertainty is derived from a calibration of the luminosity scale using a pair of x - y beam-separation scans performed in August 2015 and following a methodology similar to that detailed in Ref. [24]. In this dataset, each event includes an average of approximately 14 additional inelastic pp collisions in the same bunch crossing (in-time pile-up). The events used in this search were selected using a trigger logic that accepts events with an uncorrected missing transverse momentum above 70 GeV, calculated using a sum over calorimeter cells. Additional events selected with lepton- and photon-based triggers are employed for control

regions defined to estimate SM background contributions. All the selections employed in this paper use a highly efficient trigger selection. The triggers used are in a plateau region and the systematic uncertainties related to the trigger simulation are found to be negligible.

Monte Carlo (MC) simulated event samples are used to model the expected signal and to aid in the description and estimation of SM background processes. The response of the detector is simulated [25] either fully by a software program based on GEANT4 [26] or by a faster simulation based on a parameterization [27] for the calorimeter response and GEANT4 for the other detector systems. To account for additional pp interactions from the same and close-by bunch crossings, a set of minimum-bias interactions generated using PYTHIA [28] 8.186 and the MSTW2008LO [29,30] parton distribution function (PDF) set is superimposed onto the hard scattering events to reproduce the observed distribution of the average number of interactions per bunch crossing.

The signal samples are generated using MADGRAPH5_AMC@NLO [31] v2.2.3 interfaced to PYTHIA 8.186 with the A14 [32] set of parameters (tune) for the modelling of the parton showering (PS), hadronization and underlying event. The matrix element (ME) calculation is performed at tree level and includes the emission of up to two additional partons. The PDF set used for the generation is NNPDF23LO [33]. The ME-PS matching is done using the CKKW-L [34] prescription, with a matching scale set to one quarter of the bottom squark mass. The cross-sections used to evaluate the signal yields are calculated to next-to-leading-order accuracy in the strong coupling constant, adding the resummation of soft gluon emission at next-to-leading-logarithmic accuracy (NLO+NLL) [35–37].

SM background samples are simulated using different MC generator programs depending on the process. Events containing W or Z bosons with associated jets, including jets from the fragmentation of b - and c -quarks (heavy-flavour jets), are simulated using the SHERPA 2.1.1 [38] generator. Matrix elements are calculated for up to two additional partons at next-to-leading order (NLO) and four partons at leading order (LO) using the COMIX [39] and OPENLOOPS [40] matrix element generators and merged with the SHERPA PS [41] using the ME+PS@NLO prescription [42]. The CT10 [43] PDF set is used in conjunction with a dedicated PS tune developed by the SHERPA authors. The W/Z +jets events are normalized to their next-to-NLO (NNLO) QCD theoretical cross-sections [44]. For a cross-check of the modelling of Z +jets background, samples of events containing a photon produced in association with jets, including heavy-flavour jets, are simulated using the SHERPA 2.1.1 generator with matrix elements calculated at LO with up to four partons for the LO calculation.

Diboson processes are also simulated using the SHERPA 2.1.1 generator with the same settings as the single-boson

² ATLAS uses a right-handed coordinate system with its origin at the nominal interaction point in the centre of the detector. The positive x -axis is defined by the direction from the interaction point to the centre of the LHC ring, with the positive y -axis pointing upwards, while the beam direction defines the z -axis. Cylindrical coordinates (r, ϕ) are used in the transverse plane, ϕ being the azimuthal angle around the z -axis. The pseudorapidity η is defined in terms of the polar angle θ by $\eta = -\ln \tan(\theta/2)$. Rapidity is defined as $y = 0.5 \ln[(E + p_z)/(E - p_z)]$ where E denotes the energy and p_z is the component of the momentum along the beam direction.

samples. They are calculated for up to one (ZZ) or zero (WW , WZ) additional partons at NLO and up to three additional partons at LO. The NLO generator cross-sections are scaled down by 9 % to account for the usage of $\alpha_{\text{QED}}=1/129$ rather than $1/132$, the latter corresponding to the use of the parameters defined by the Particle Data Group as input to the G_μ scheme [45].

Top-quark pair and single-top-quark production (Wt - and s -channel) events are simulated using the POWHEG-BOX v2 [46] generator as described in Ref. [47] with the CT10 PDF set in the matrix element calculations. Electroweak t -channel single-top-quark events are generated using the POWHEG-BOX v1 generator. The top-quark mass is set to 172.5 GeV. For the $t\bar{t}$ production, the h_{damp} parameter, which controls the transverse momentum (p_T) of the first additional emission beyond the Born configuration and thus regulates the p_T of the recoil emission against the $t\bar{t}$ system, is set to the mass of the top quark. For all processes, the parton shower, fragmentation, and the underlying event are simulated using PYTHIA 6.428 [48] with the CTEQ6L1 PDF set and the corresponding Perugia 2012 tune (P2012) [49]. The $t\bar{t}$ samples are normalized to their NNLO cross-section including the resummation of soft gluon emission at next-to-NLL accuracy using $\text{Top}++2.0$ [50]. Samples of single-top-quark production are normalized to the NLO cross-sections reported in Refs. [51–53] for the s -, t - and Wt -channels, respectively. The associated production of a top-quark pair with a vector boson, $t\bar{t}+W/Z$, is generated at LO with MADGRAPH5_AMC@NLO v2.2.3 interfaced to PYTHIA 8.186, with up to two ($t\bar{t}+W$), one ($t\bar{t}+Z$) or no ($t\bar{t}+WW$) extra partons included in the matrix elements. The samples are normalized to their NLO cross-sections [31].

The EvtGen 1.2.0 program [54] is used for modelling the properties of bottom- and charm-hadron decays in all samples generated with MADGRAPH5_AMC@NLO and POWHEG-BOX.

Several samples produced without detector simulation are employed to derive systematic uncertainties associated with the specific configuration of the MC generators used for the nominal SM background samples. They include variations of the renormalization and factorization scales, the CKKW-L matching scale, as well as different PDF sets and fragmentation/hadronization models. Details of the MC modelling uncertainties are discussed in Sect. 7.

4 Event reconstruction

The search for bottom squark pair production is based on a selection of events with jets and large missing transverse momentum in the final state. Events containing electrons or muons are explicitly vetoed in the signal and validation regions, and are used to define control regions. An overlap

removal procedure is applied to prevent double-counting of reconstructed objects. The details of the selections and overlap removal are given below.

Interaction vertices from the pp collisions are reconstructed from tracks in the inner detector. Events must have at least one primary reconstructed vertex, required to be consistent with the beamspot envelope and to consist of at least two tracks with $p_T > 0.4$ GeV. When more than one such vertex is found the one with the largest sum of the square of transverse momenta of associated tracks [55] is chosen.

Jet candidates are reconstructed from three-dimensional energy clusters [56] in the calorimeter using the anti- k_t jet algorithm [57] with a radius parameter of 0.4. Each topological cluster's energy is calibrated to the electromagnetic scale prior to jet reconstruction. The reconstructed jets are then calibrated to the particle level by applying a jet energy scale (JES) derived from simulation and *in situ* corrections based on 8 TeV data [58,59]. Quality criteria are imposed to identify jets arising from non-collision sources or detector noise and any event containing such a jet is removed [60]. Further track-based selections are applied to reject jets with $p_T < 60$ GeV and $|\eta| < 2.4$ that originate from pile-up interactions [61] and the expected event average energy contribution from pile-up clusters is subtracted using a factor dependent on the jet area [58]. Jets are classified as “baseline” and “signal”. Baseline jets are required to have $p_T > 20$ GeV and $|\eta| < 2.8$. Signal jets, selected after resolving overlaps with electrons and muons, are required to pass the stricter requirement of $p_T > 35$ GeV.

Jets are identified as b -jets if tagged by a multivariate algorithm which uses information about the impact parameters of inner detector tracks matched to the jet, the presence of displaced secondary vertices, and the reconstructed flight paths of b - and c -hadrons inside the jet [62]. The b -tagging working point with a 77 % efficiency, as determined in a simulated sample of $t\bar{t}$ events, was chosen as part of the optimization process discussed in Sect. 5. The corresponding rejection factors against jets originating from c -quarks and from light quarks and gluons at this working point are 4.5 and 130, respectively [63]. To compensate for differences between data and MC simulation in the b -tagging efficiencies and mis-tag rates, correction factors derived from data-driven methods are applied to the simulated samples [64]. Candidate b -tagged jets are required to have $p_T > 50$ GeV and $|\eta| < 2.5$.

Electron candidates are reconstructed from energy clusters in the electromagnetic calorimeter matched to a track in the inner detector and are required to satisfy a set of “loose” quality criteria [65–67]. They are also required to lie within the fiducial volume $|\eta| < 2.47$. Muon candidates are reconstructed from matching tracks in the inner detector and the muon spectrometer. Events containing one or more muon candidates that have a transverse (longitudinal) impact

parameter with respect to the primary vertex larger than 0.2 mm (1 mm) are rejected to suppress cosmic rays. Muon candidates are also required to satisfy “medium” quality criteria [68] and have $|\eta| < 2.5$. All electron and muon candidates must have $p_T > 10$ GeV. Lepton candidates remaining after resolving the overlap with baseline jets (see next paragraph) are called “baseline” leptons. In the control regions where lepton identification is required, “signal” leptons are chosen from the baseline set with $p_T > 26$ GeV to ensure full efficiency of the trigger and are required to be isolated from other activity using a selection designed to accept 99 % of leptons from Z boson decays. Signal electrons are further required to satisfy “tight” quality criteria [65]. Electrons (muons) are matched to the primary vertex by requiring the transverse impact parameter (d_0) to satisfy $|d_0/\sigma(d_0)| < 5$ (3), and the longitudinal impact parameter (z_0) to satisfy $|z_0 \sin \theta| < 0.5$ mm for both the electrons and muons. The MC events are corrected to account for differences in the lepton trigger, reconstruction and identification efficiencies between data and MC simulation.

The sequence to resolve overlapping objects begins by removing electron candidates sharing an inner detector track with a muon candidate. Next, jet candidates within $\Delta R = \sqrt{(\Delta y)^2 + (\Delta \phi)^2} = 0.2$ of an electron candidate are discarded, unless the jet is b -tagged, in which case the electron is discarded since it is likely to originate from a semileptonic b -hadron decay. Finally, any lepton candidate remaining within $\Delta R = 0.4$ of any surviving jet candidate is discarded, except for the case where the lepton is a muon and the number of tracks associated with the jet is less than three.

The missing transverse momentum $\mathbf{p}_T^{\text{miss}}$, with magnitude E_T^{miss} , is defined as the negative vector sum of the p_T of all selected and calibrated physics objects in the event, with an extra term added to account for soft energy in the event which is not associated with any of the selected objects. This soft term is calculated from inner detector tracks with p_T above 400 MeV matched to the primary vertex to make it more robust against pile-up contamination [69,70].

Reconstructed photons, although not used in the main signal event selection, are selected in the regions employed in one of the alternative methods used to check the Z +jets background, as explained in Sect. 6. Photon candidates are required to have $p_T > 130$ GeV and $|\eta| < 2.37$, to satisfy the tight photon shower shape and electron rejection criteria [71], and to be isolated.

5 Event selection

The selection of events is similar to that used in Ref. [72] and is based on the definition of one set of three overlapping signal regions (SRA) and a fourth distinct signal region (SRB). These were re-optimized for 3.2 fb^{-1} of 13 TeV pp colli-

Table 1 Summary of the event selection in each signal region. The term lepton is used in the table to refer to baseline electrons and muons. Jets (j_1, j_2, j_3 and j_4) are labelled with an index corresponding to their decreasing order in p_T

Variable	SRA	SRB
Event cleaning	Common to all SR	
Lepton veto	No e/μ with $p_T > 10$ GeV after overlap removal	
E_T^{miss} (GeV)	> 250	> 400
$n(\text{jets})$ $p_T > 35$ GeV	2–4	3–4
1st jet $p_T(j_1)$ (GeV)	> 130	> 300
2nd jet $p_T(j_2)$ (GeV)	> 50	> 50
4th jet	Vetoed if $p_T(j_4) > 50$ GeV	
$\Delta \phi_{\min}^j$	> 0.4	> 0.4
$\Delta \phi(j_1, E_T^{\text{miss}})$	–	> 2.5
b -tagging	j_1 and j_2	j_2 and (j_3 or j_4)
$E_T^{\text{miss}}/m_{\text{eff}}$	> 0.25	> 0.25
m_{CT} (GeV)	$> 250, 350, 450$	–
m_{bb} (GeV)	> 200	–

sions, and the selection criteria are summarized in Table 1. Only events with $E_T^{\text{miss}} > 250$ GeV are retained to ensure full efficiency of the trigger. Jets are ordered according to decreasing p_T . Contamination from backgrounds with high jet multiplicity, particularly $t\bar{t}$ production, is suppressed by vetoing events with a fourth jet with $p_T > 50$ GeV. To discriminate against multijet background, events where E_T^{miss} is aligned with a jet in the transverse plane are rejected by requiring $\Delta \phi_{\min}^j > 0.4$, where $\Delta \phi_{\min}^j$ is the minimum azimuthal distance between E_T^{miss} and the leading four jets, and by requiring $E_T^{\text{miss}}/m_{\text{eff}} > 0.25$, where m_{eff} is defined as the scalar sum of the E_T^{miss} and the p_T of the two leading jets. For signal events, no isolated charged leptons are expected in the final state, and events where a baseline electron or muon is reconstructed are discarded.

The first set of signal regions, SRA, selects events with large E_T^{miss} where the two leading jets are b -tagged to target models with a large mass difference between the bottom squark and the neutralino. The main discriminating variable is the contranverse mass (m_{CT}) [73], which is a kinematic variable that can be used to measure the masses of pair-produced semi-invisibly decaying heavy particles. For two identical decays of heavy particles into two visible particles (or particle aggregates) v_1 and v_2 , and two invisible particles, m_{CT} is defined as

$$m_{CT}^2(v_1, v_2) = [E_T(v_1) + E_T(v_2)]^2 - [\mathbf{p}_T(v_1) - \mathbf{p}_T(v_2)]^2.$$

In this analysis, v_1 and v_2 are the two leading b -jets. For signal events, these correspond to the b -jets from the squark decays and the invisible particles are the two neutralinos.

The contranverse mass is invariant under equal and opposite boosts of the parent particles in the transverse plane. For systems of parent particles produced with small transverse boosts, m_{CT} is bounded from above by an analytical combination of particle masses. This bound is saturated when the two visible objects are collinear. For $t\bar{t}$ events, this kinematic bound is at 135 GeV, while for production of bottom squark pairs the bound is given by $m_{CT}^{\max} = (m_{\tilde{b}_1}^2 - m_{\tilde{\chi}_1^0}^2)/m_{\tilde{b}_1}$. The selection on m_{CT} is optimized based on the bottom squark and neutralino masses considered and SRA is further divided into three overlapping regions, SRA250, SRA350 and SRA450, where the naming conventions reflects the minimum value allowed for m_{CT} . Finally, a selection on the invariant mass of the two b -jets ($m_{bb} > 200$ GeV) is applied to further enhance the signal yield over the SM background contributions. For a signal model corresponding to $m_{\tilde{b}_1} = 800$ GeV and $m_{\tilde{\chi}_1^0} = 1$ GeV, 10, 8 and 5 % of the simulated signal events are retained by the SRA250, SRA350 and SRA450 selections, respectively.

The second type of signal region, SRB, selects events where a bottom squark pair is produced in association with a jet from initial-state radiation (ISR). The SRB targets models with a small mass difference between the \tilde{b}_1 and the $\tilde{\chi}_1^0$, such that a boosted bottom squark pair is needed to satisfy the trigger requirements. Hence events are selected with large E_T^{miss} , one high- p_T non- b -tagged leading jet and at least two additional b -jets. The leading jet is also required to be pointing in the direction opposite to the E_T^{miss} by requiring $\Delta\phi(j_1, E_T^{\text{miss}}) > 2.5$, where $\Delta\phi(j_1, E_T^{\text{miss}})$ is defined as the azimuthal angle between the leading jet and the E_T^{miss} . For a signal model corresponding to $m_{\tilde{b}_1} = 400$ GeV and $m_{\tilde{\chi}_1^0} = 300$ GeV, about 0.3 % of the simulated events are retained by the SRB selection.

6 Background estimation

The dominant SM background processes in the signal regions are the production of W or Z bosons in association with heavy-flavour jets (referred to as W +hf and Z +hf) and the production of top quarks. In particular, events with Z +hf production followed by the $Z \rightarrow \nu\bar{\nu}$ decay have the same signature as the signal and are the largest (irreducible) background in SRA. The background in SRB is dominated by top-quark production in events with a charged lepton in the final state that is not reconstructed, either because the lepton is a hadronically decaying τ , or because the electron or muon is not identified or out of detector acceptance.

Monte Carlo simulation is used to estimate the background yield in the signal regions, after normalizing the Monte Carlo prediction for the major backgrounds to data in control

regions (CR) constructed to enhance a particular background and to be kinematically similar but orthogonal to the signal regions. The control regions are defined by explicitly requiring the presence of one or two leptons (electrons or muons) in the final state and applying further selection criteria similar to those of the corresponding signal regions. To select events with good-quality electrons and muons the “signal lepton” selection is applied to them. Events with additional baseline lepton candidates are vetoed. For SRA, the normalizations of the top-quark pair, single-top-quark, Z +jets and W +jets backgrounds are estimated simultaneously by making use of four control regions, while for SRB two control regions are used to determine the normalization of the top-quark pair and Z +jets backgrounds since other contributions are sub-dominant. A likelihood function is built as the product of Poisson probability functions, using as constraints the observed and expected (from MC simulation) event yields in the control regions but not the yields in the corresponding SR [74]. The normalization factors for each of the simulated backgrounds are adjusted simultaneously via a profile likelihood fit [75] (referred to as the “background-only fit”). All systematic uncertainties (discussed in Sect. 7) are treated as nuisance parameters in the fit. The background normalization parameters are applied to the signal regions also taking into account correlations in the yield predictions between different regions.

Two same-flavour opposite-sign (SFOS) two-lepton (electron or muon) control regions with dilepton invariant mass near the Z boson mass ($76 < m_{\ell\ell} < 106$ GeV) and two b -tagged jets provide data samples dominated by Z boson production. For these control regions, labelled in the following as CRzA and CRzB for SRA and SRB respectively, the p_T of the leptons is added vectorially to the \vec{p}_T^{miss} to mimic the expected missing transverse momentum spectrum of $Z \rightarrow \nu\bar{\nu}$ events, and is indicated in the following as $E_T^{\text{miss,cor}}$ (lepton corrected). In addition, the uncorrected E_T^{miss} of the event is required to be less than 100 (70) GeV in CRzA (CRzB) in order to further enhance the Z boson contribution. In the case of CRzA, a $m_{bb} > 200$ GeV selection is also imposed. Two control regions, CRttA and CRttB defined for SRA and SRB respectively, dominated by $t\bar{t}$ production are identified by selecting events with exactly one lepton (e, μ) and a set of requirements similar to those for SRA and SRB, with the additional requirement $m_{bb} < 200$ GeV in CRttA to separate the $t\bar{t}$ pair contribution from single top-quark production. To assist in the estimation of the background from W +hf and single top-quark production in SRA two further one-lepton control regions (CRwA and CRstA) are defined. These control regions exploit kinematic features to differentiate these processes from $t\bar{t}$ production. For CRstA a selection is applied to the minimum invariant mass of either of the b -jets and the charged lepton ($m_{b\ell}^{\min}$). For CRwA only one b -jet

Table 2 Definition of the control regions associated with SRA and SRB. Control regions are defined to study the contribution from $Z+hf$, $t\bar{t}$, single top-quark and $W+hf$ production in SRA and the contribution from $Z+hf$ and $t\bar{t}$ in SRB. The term lepton is used in the table to refer

to signal electrons and muons. Jets (j_1 , j_2 , j_3 and j_4) are labelled with an index corresponding to their decreasing order in p_T . SFOS indicates the same-flavour opposite-sign two-lepton selection

Variable	CRzA	CRttA	CRstA	CRwA	CRzB	CRttB
Number of leptons	2 SFOS	1	1	1	2 SFOS	1
1st lepton p_T (GeV)	>90	>26	>26	>26	>26	>26
2nd lepton p_T (GeV)	>20	–	–	–	>20	–
$m_{\ell\ell}$ (GeV)	[76, 106]	–	–	–	[76, 106]	–
m_T (GeV)	–	–	–	>30	–	–
$n(\text{jets})$ $p_T > 35$ GeV	2–4	2–4	2–4	2–4	3–4	3–4
1st jet $p_T(j_1)$ (GeV)	>50	>130	>50	>130	>50	>130
2nd jet $p_T(j_2)$ (GeV)	>50	>50	>50	>50	>50	>50
4th jet	Vetoed if $p_T(j_4) > 50$ GeV				Vetoed if $p_T(j_4) > 50$ GeV	
b -tagged jets	j_1 and j_2	j_1 and j_2	j_1 and j_2	j_1	j_2 and (j_3 or j_4)	
E_T^{miss} (GeV)	<100	>100	>100	>100	<70	>200
$E_T^{\text{miss,cor}}$ (GeV)	>100	–	–	–	>100	–
m_{bb} (GeV)	>200	<200	>200	$(m_{bj}) > 200$	–	–
m_{CT} (GeV)	–	>150	>150	>150	–	–
$m_{b\ell}^{\text{min}}$ (GeV)	–	–	>170	–	–	–
$\Delta\phi(j_1, E_T^{\text{miss}})$	–	–	–	–	>2.0	>2.5

is required, the selection on m_{bb} is replaced by a selection on the invariant mass of the two leading jets (m_{bj}) and a further selection is applied to the event transverse mass m_T , defined as $m_T = \sqrt{2p_T^{\text{lep}} E_T^{\text{miss}} - 2\mathbf{p}_T^{\text{lep}} \cdot \mathbf{p}_T^{\text{miss}}}$. The definitions of the control regions are summarized in Table 2.

The contributions from diboson and $t\bar{t} + W/Z$ processes are minor and they are collectively called “Others” in the following. They are estimated from MC simulation for both the signal and the control regions and included in the fit procedure, and are allowed to vary within their uncertainty. The background from multijet production is estimated from data using a procedure described in detail in Ref. [76] and modified to account for the flavour of the jets. The procedure consists of smearing the jet response in events with well-measured E_T^{miss} (seed events). The jet response function is obtained from MC dijet events and cross-checked in events from data where the E_T^{miss} can be unambiguously attributed to the mis-measurement of one of the jets. The contribution from multijet production in all regions is found to be negligible.

The results of the background-only fit are shown in Table 3, where the contribution from individual backgrounds is shown separately as a purely MC-based prediction and with the rescaling from the fit procedure. The m_{bb} distribution in CRzA and the p_T of the leading jet in CRttB are shown in Fig. 1 after the backgrounds were rescaled as a result of the background-only fit, showing good agreement in the shape of the distributions in the two control regions used to estimate the dominant backgrounds in SRA and SRB.

The full background estimation procedure is validated by comparing the background predictions and the shapes of the distributions of the key analysis variables from the fit results to those observed in dedicated validation regions. They are defined to be mutually exclusive and kinematically similar to the signal regions, with low potential contamination from signal. For SRA, two validation regions are defined by using the same definition as SRA250, and inverting the selections on m_{bb} and m_{CT} . The SM predictions are found to overestimate the data by about one standard deviation. For SRB, a validation region is defined by selecting events with $250 < E_T^{\text{miss}} < 300$ GeV and good agreement is observed between data and predictions.

As a further validation, two alternative methods are used to estimate the $Z+hf$ contribution. The first method exploits the similarity of the Z -jets and γ -jets processes [76]. For p_T of the photon significantly larger than the mass of the Z boson, the kinematics of γ -jets events strongly resemble those of Z -jets events. The event yields are measured in control regions identical to the SRA and SRB, with the E_T^{miss} -based selections replaced by selections on the p_T of the photon vectorially added to the $\mathbf{p}_T^{\text{miss}}$. The yields are then propagated to the actual SRA and SRB using a reweighting factor derived using the MC simulation. This factor takes into account the different kinematics of the two processes and residual effects arising from the acceptance and reconstruction efficiency for photons.

In the second alternative method, applied to SRA only where the $Z+hf$ contribution is dominant, the MC simulation

Table 3 Fit results in the control regions associated with the SRA and SRB selection for an integrated luminosity of 3.2 fb^{-1} . The results are obtained from the control regions using the background-only fit. The uncertainties include statistical, detector-related and theoretical systematic components. The individual uncertainties can be correlated and do

not necessarily add in quadrature to the total systematic uncertainty. The pure MC estimate is used for backgrounds for which a dedicated CR is not defined, e.g. for smaller backgrounds (indicated as “Other”) and for single top-quark and W +jets production in CRzB and CRttB. A dash indicates a negligible background

Control region	CRzA	CRwA	CRttA	CRstA	CRzB	CRttB
Observed	78	543	260	56	59	188
Total background (fit)	78 ± 9	543 ± 23	260 ± 16	56 ± 7	59 ± 8	188 ± 14
$t\bar{t}$	9.0 ± 1.6	153 ± 26	181 ± 23	11.1 ± 2.1	14.6 ± 2.0	156 ± 15
Single top	0.8 ± 0.4	50 ± 23	27 ± 13	23 ± 10	0.42 ± 0.07	16.6 ± 2.0
W +jets	–	327 ± 43	45 ± 14	20 ± 6	–	13 ± 5
Z +jets	68 ± 9	3.8 ± 0.6	1.4 ± 0.2	0.9 ± 0.2	42 ± 8	0.3 ± 0.1
“Other”	0.9 ± 0.1	8.1 ± 1.1	5.8 ± 0.7	0.6 ± 0.1	1.6 ± 0.4	2.3 ± 0.2
Total background (MC exp.)	61	503	267	57	46	191
$t\bar{t}$	9.4	161	190	12	15	159
Single top	1.1	60	33	27	0.4	16
W +jets	–	270	37	17	–	12.9
Z +jets	50	2.8	1.0	0.7	29	0.2
“Other”	0.9	8.1	5.8	0.6	1.6	2.3

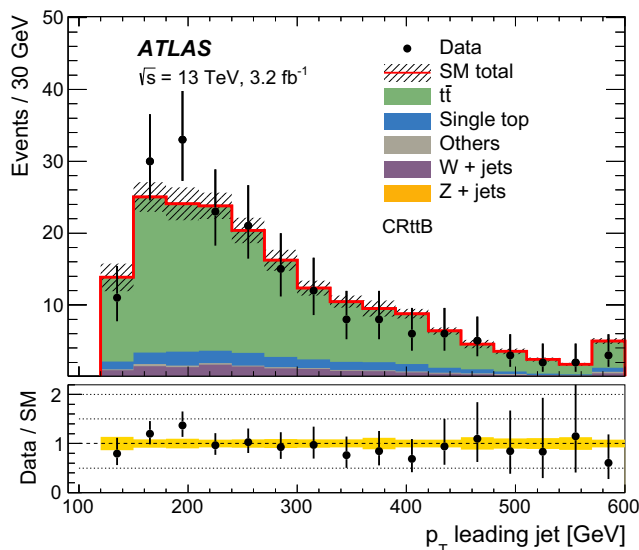
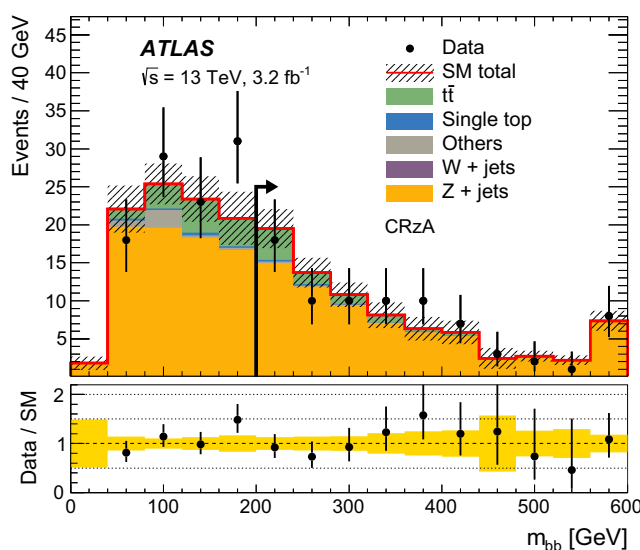


Fig. 1 Left m_{bb} distribution in CRzA before the final selection $m_{bb} > 200 \text{ GeV}$ is applied (indicated by the arrow). Right p_T of the leading jet in CRttB. In both distributions the MC normalization is rescaled using the results from the background-only fit, showing good agreement

between data and the predicted SM shapes. The shaded band includes statistical and detector-related systematic uncertainties as detailed in Sect. 7 and the last bin includes overflows

is used to verify that the shape of the m_{CT} distribution for events with no b -tagged jets is compatible with the shape of the m_{CT} distribution for events where two b -tagged jets are present. A new highly populated Z +jets CR is defined selecting $Z \rightarrow \ell\ell$ events with no b -tagged jets. The m_{CT} distribution in this CR is constructed using the two leading jets and is used to estimate the shape of the m_{CT} distribution in the SRA, whilst the normalization in SRA is rescaled based

on the ratio in data of $Z \rightarrow \ell\ell$ events with no b -tagged jets to events with two b -tagged jets. Additional MC-based corrections are applied to take into account the two-lepton selection in this CR.

The two alternative methods are in agreement within uncertainties with the estimates obtained with the profile likelihood fit to the control regions (Table 4). Experimental and theoretical systematic uncertainties in the nominal

Table 4 Estimated Z+jets yields in the signal regions as obtained using the default and the two alternative methods. The errors include all the uncertainty sources discussed in Sect. 7. The “MC-based post-fit” uncer-

tainty does not include the additional uncertainty to account for the difference between the three methods

Method\region	SRA250	SRA350	SRA450	SRB
Nominal MC-based post-fit	22 ± 4	5.0 ± 0.9	1.3 ± 0.3	4.1 ± 0.9
Z+jets from γ +jets events	18 ± 5	3.7 ± 1.5	1.8 ± 1.0	2.2 ± 1.0
Z+jets from non b -tagged Z events	18 ± 6	4.3 ± 1.6	1.3 ± 0.5	Not applicable

Table 5 Summary of the dominant experimental and theoretical uncertainties for each signal region. Uncertainties are quoted as relative to the total uncertainty, with a range indicated for the three SRAs. For theoretical modelling, uncertainties per dominant SM background process are quoted. The individual uncertainties can be correlated, and do not necessarily add in quadrature to the total background uncertainty

Source\region	SRA (%)	SRB (%)
Experimental uncertainty		
JES	15–30	25
JER	20–35	<10
b -tagging	25–45	15
Theoretical modelling uncertainty		
Z+jets	25–35	12
W+jets	20–22	27
Top production	15–20	70

and alternative method estimates are taken into account (see Sect. 7). The difference between the alternative methods and the background-only fit is taken into account as an additional systematic uncertainty in the final Z+hf yields.

7 Systematic uncertainties

Several sources of experimental and theoretical systematic uncertainty are considered in this analysis. Their impact is reduced through the normalization of the dominant backgrounds in the control regions with kinematic selections resembling those of the corresponding signal region (see Sect. 6). Uncertainties due to the limited number of events in the CRs are also taken into account in the fit. The individual contributions are outlined in Table 5.

The dominant detector-related systematic effects are due to the uncertainties in the jet energy scale (JES) [58] and resolution (JER) [59], and in the b -tagging efficiency and mis-tagging rates. The JES and JER uncertainties are estimated from 13 TeV data, while the uncertainties related to b -tagging are estimated from 8 TeV data and extrapolated to 13 TeV and to the Run-2 detector conditions. The uncertainties associated with lepton and photon reconstruction and energy measurements are also considered but have a small

impact on the final results. Lepton, photon and jet-related uncertainties are propagated to the calculation of the E_T^{miss} , and additional uncertainties are included in the energy scale and resolution of the soft term. The overall experimental uncertainty in the SM background estimate is found to be around 20 % for the SRAs and 15 % for the SRB.

Uncertainties in the modelling of the SM background processes from MC simulation and their theoretical cross-section uncertainties are also taken into account. The dominant uncertainty arises from Z+jets MC modelling for SRA and $t\bar{t}$ modelling for SRB. The Z+jets (as well as W+jets) modelling uncertainties are evaluated using alternative samples generated with different renormalization and factorization scales, merging (CKKW-L) and resummation scales. An additional one-sided uncertainty in the Z+jets estimate is taken as the largest deviation between the nominal background-only fit result and each of the alternative data-driven estimates described in Sect. 6. This results in an additional 25, 25 and 40 % one-sided uncertainty in SRA250, SRA350 and SRA450, respectively. Finally, a 40 % uncertainty [77] is assigned to the heavy-flavour jet content in W+jets, estimated from MC simulation in SRB. For SRA, the uncertainty accounts for the different requirements on b -jets between CRwA and the signal region.

Uncertainties in the modelling of the top-quark pair and single-top-quark (Wt) backgrounds are sub-dominant in SRA and dominant in SRB. They are computed as the difference between the predictions from nominal samples and those of additional samples differing in generator or parameter settings. Hadronization and PS uncertainties are estimated using samples generated with POWHEG-BOX v2 and showered by HERWIG++ v2.7.1 [78] with the UEEE5 underlying event tune. Uncertainties related to initial- and final-state radiation modelling, tune and (for $t\bar{t}$ only) choice of h_{damp} parameter in POWHEG-BOX v2 are evaluated using alternative settings of the generators. Finally, an alternative generator MADGRAPH5_AMC@NLO with showering by HERWIG++ v2.7.1 is used to estimate the generator uncertainties. Uncertainties in smaller backgrounds such as diboson and ttV are also estimated by comparisons of the nominal sample with alternative samples differing in generator or parameter settings (POWHEG v2 with showering by PYTHIA 8.210 for diboson, renormalization and factorization scale and A14

Table 6 Fit results in all signal regions for an integrated luminosity of 3.2 fb^{-1} . The results are obtained from the control regions. The background normalization parameters obtained with the background-only fit are applied to the SRs. The individual uncertainties, including detector-related and theoretical systematic components, are symmetrized and can be correlated and do not necessarily add in quadrature to the total systematic uncertainty

Signal region	SRA250	SRA350	SRA450	SRB
Observed	23	6	1	6
Total background (fit)	29 ± 5	7.0 ± 1.2	1.8 ± 0.4	12.0 ± 2.5
$t\bar{t}$	1.0 ± 0.4	0.17 ± 0.08	0.04 ± 0.02	5.5 ± 2.0
Single top	1.8 ± 1.0	0.53 ± 0.30	0.13 ± 0.07	1.0 ± 0.4
W+jets	4.4 ± 1.3	1.2 ± 0.4	0.30 ± 0.10	1.1 ± 0.6
Z+jets	22 ± 4	5.0 ± 1.1	1.3 ± 0.4	4.1 ± 1.3
“Other”	0.45 ± 0.06	0.14 ± 0.04	0.04 ± 0.04	0.3 ± 0.1
Total background (MC exp.)	23	5.6	1.5	11
$t\bar{t}$	1.1	0.18	0.04	5.6
Single top	2.2	0.6	0.15	1.0
W+jets	3.6	1.0	0.25	1.1
Z+jets	16	3.7	1.0	2.8
“Other”	0.45	0.14	0.04	0.3

tune variations for ttV) and are found to be negligible. The cross-sections used to normalize the MC yields to the highest order available are varied according to the scale uncertainty of the theoretical calculation, i.e. 5 % for W, Z boson and top-quark pair production, 6 % for diboson, 13 and 12 % for ttW and ttZ , respectively.

For the SUSY signal processes, both the experimental and theoretical uncertainties in the expected signal yield are considered. Experimental uncertainties, which are found to be between 20 and 25 % across the $\tilde{b}_1 - \tilde{\chi}_1^0$ mass plane for all SRs, are largely dominated by the uncertainty in the b -tagging efficiency in SRA, while JER and b -tagging uncertainties are dominant in SRB with equal contributions. Theoretical uncertainties in the NLO+NLL cross-section are calculated for each SUSY signal scenario and are dominated by the uncertainties in the renormalization and factorization scales, followed by the uncertainty in the PDF. They vary between 15 and 20 % for bottom squark masses in the range between 400 and 900 GeV. Additional uncertainties in the modelling of initial-state radiation in SUSY signal MC samples are taken into account and contribute up to 5 %.

8 Results and interpretation

Table 6 reports the observed number of events and the SM predictions after the background-only fit for each signal region. The largest background contribution in SRA arises from $Z \rightarrow \nu\bar{\nu}$ produced in association with b -quarks whilst top-quark pair production dominates SM predictions for SRB. The background-only fit results are compared to the pre-fit predictions based on MC simulation. Figures 2 and 3 show the comparison between the observed data and the SM predictions for some relevant kinematic distributions in SRA250 and SRB, respectively, prior to the selec-

tion on the variable shown. For illustrative purposes, the distributions expected for a scenario with bottom squark and neutralino masses of 700 GeV (400 GeV) and 1 GeV (300 GeV), respectively, are shown for SRA250 (SRB). No excess above the expected Standard Model background yield is observed. The results are translated into upper limits on contributions from new physics beyond the SM (BSM) for each signal region. The CL_s method [79, 80] is used to derive the confidence level of the exclusion; signal models with a CL_s value below 0.05 are said to be excluded at 95 % CL. The profile-likelihood-ratio test statistic is used to exclude the signal-plus-background hypothesis for specific signal models. When normalized by the integrated luminosity of the data sample, results can be interpreted as corresponding upper limits on the visible cross-section, σ_{vis} , defined as the product of the BSM production cross-section, the acceptance and the selection efficiency of a BSM signal. Table 7 summarizes the observed (S_{obs}^{95}) and expected (S_{exp}^{95}) 95 % CL upper limits on the number of BSM events and on σ_{vis} .

Exclusion limits are obtained assuming a specific SUSY particle mass hierarchy such that the lightest bottom squark decays exclusively via $\tilde{b}_1 \rightarrow b\tilde{\chi}_1^0$. In this case, the fit procedure takes into account not only correlations in the yield predictions between control and signal regions due to common background normalization parameters and systematic uncertainties but also contamination in the control regions from SUSY signal events (found to be generally negligible). The experimental systematic uncertainties in the signal are taken into account for this calculation and are assumed to be fully correlated with those in the SM background. Figure 4 shows the observed (solid line) and expected (dashed line) exclusion contours at 95 % CL in the $\tilde{b}_1 - \tilde{\chi}_1^0$ mass plane.

At each point of the parameter space, the SR with the best expected sensitivity is adopted. Sensitivity to scenarios with the largest mass difference between the \tilde{b}_1 and

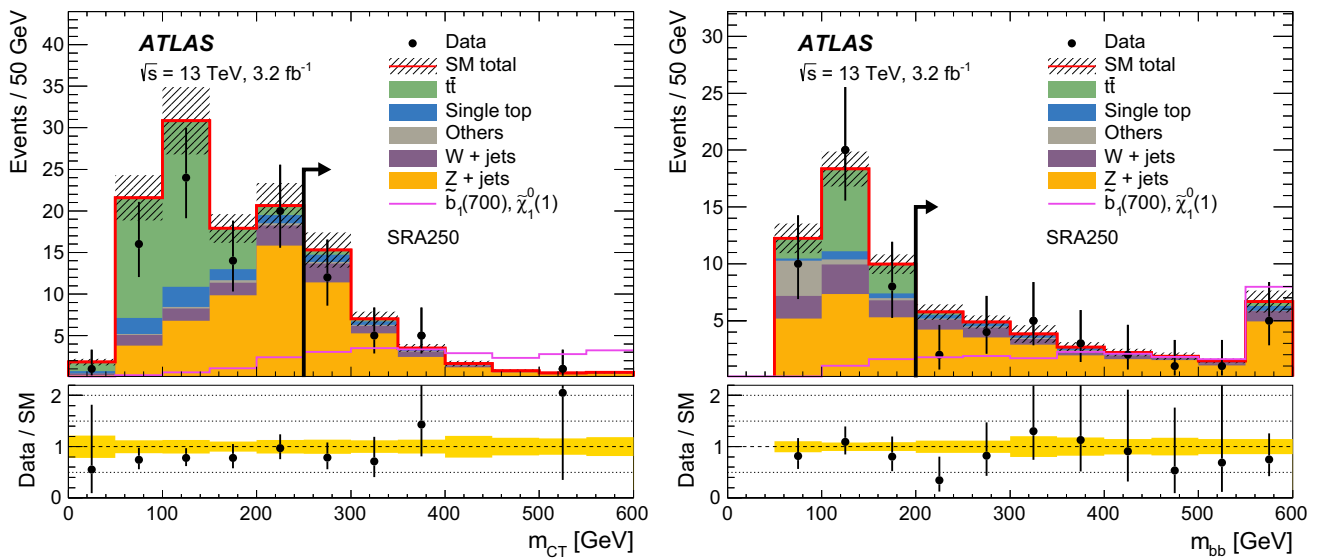


Fig. 2 *Left* m_{CT} distribution in SRA250 with all the selection criteria applied except the m_{CT} threshold. *Right* m_{bb} distribution in SRA250 with all selection criteria applied except the m_{bb} requirement. The arrows indicate the final applied selection. The shaded band includes statistical and detector-related systematic uncertainties. The SM back-

grounds are normalized to the values determined in the fit. For illustration the distributions expected for one signal model with *bottom squark* and neutralino masses of 700 and 1 GeV, respectively, are overlaid. The last bin includes overflows

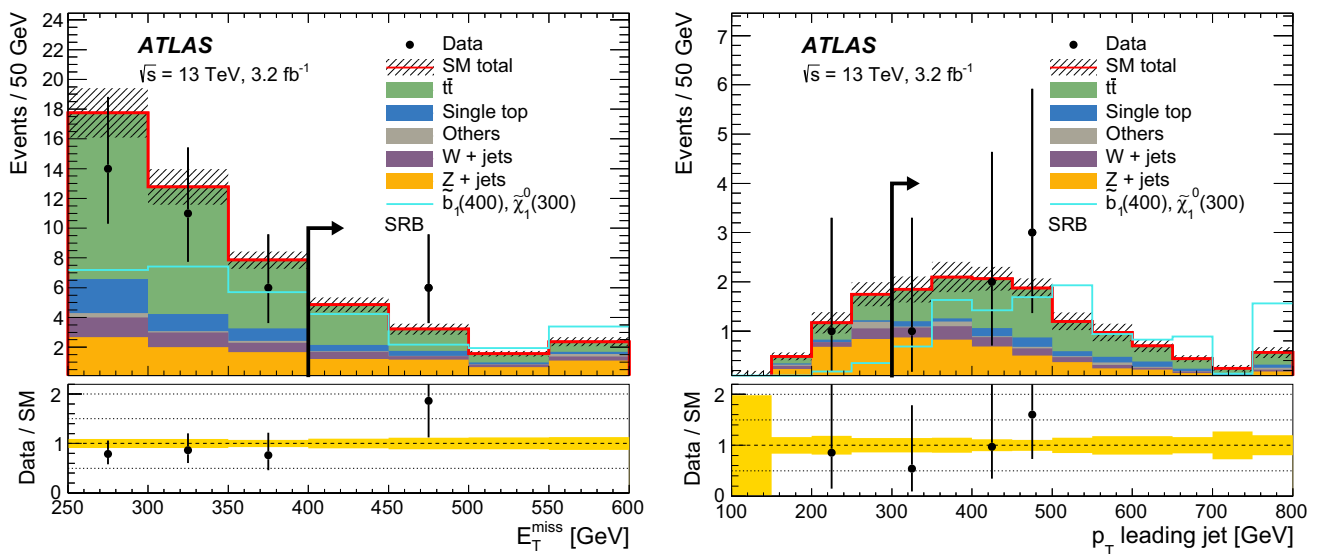


Fig. 3 *Left* E_T^{miss} distribution in SRB with all the selection criteria applied except the E_T^{miss} threshold. *Right* leading jet p_T distribution in SRB with all the selection criteria applied except the selection on the leading jet p_T itself. The arrows indicate the final selection applied in

SRB. The shaded band includes statistical and detector-related systematic uncertainties. The SM backgrounds are normalized to the values determined in the fit. For illustration the distributions expected for one signal model with *bottom squark* and neutralino masses of 400 and 300 GeV, respectively, are overlaid. The last bin includes overflows

the $\tilde{\chi}_1^0$ is achieved with the most stringent m_{CT} threshold (SRA450). Sensitivity to scenarios with smaller mass differences is achieved predominantly with searches based on the presence of a high- p_T ISR jet, as in the dedicated SRB selection and the search described in Ref. [81]. Bottom squark masses up to 800 (840) GeV are excluded for $\tilde{\chi}_1^0$ masses below 360 (100) GeV. Differences in mass above 100 GeV

between \tilde{b}_1 and $\tilde{\chi}_1^0$ are excluded up to \tilde{b}_1 masses of 500 GeV. The expected exclusion constraints are about 20 GeV lower than the observation for high bottom squark masses and about 60 GeV lower for SUSY models with small $\tilde{b}_1 - \tilde{\chi}_1^0$ mass splitting. The current results significantly extend the $\sqrt{s} = 8$ TeV limits [72, 81] despite the lower integrated luminosity mostly because of the increase in centre-of-mass energy of the LHC.

Table 7 Left to right: 95 % CL upper limits on the visible cross-section ($\langle \epsilon A \sigma \rangle_{\text{obs}}^{95}$) and on the number of signal events (S_{obs}^{95}). The third column (S_{exp}^{95}) shows the 95 % CL upper limit on the number of signal events, given the expected number (and $\pm 1\sigma$ variations of the expectation) of background events

Signal channel	$\langle \epsilon A \sigma \rangle_{\text{obs}}^{95}$ (fb)	S_{obs}^{95}	S_{exp}^{95}
SRA250	3.42	11.0	$13.8^{+6.0}_{-3.2}$
SRA350	1.93	6.2	$6.6^{+3.1}_{-1.1}$
SRA450	1.23	3.9	$4.1^{+1.9}_{-0.6}$
SRB	1.89	6.1	$8.7^{+3.1}_{-2.5}$

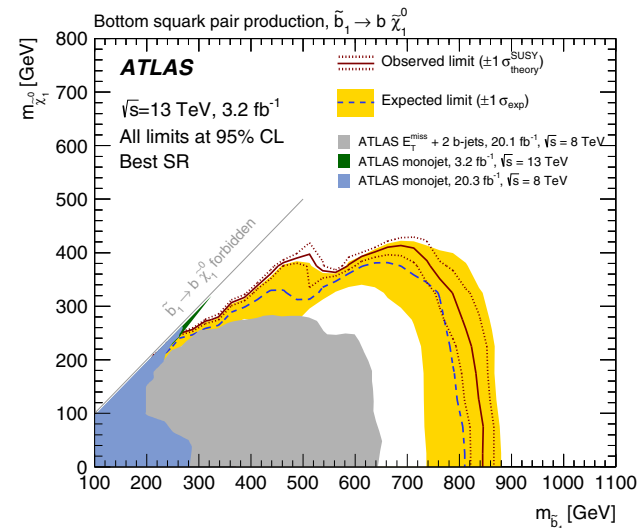


Fig. 4 Observed and expected exclusion limits at 95 % CL, as well as $\pm 1\sigma$ variation of the expected limit, in the \tilde{b}_1 - $\tilde{\chi}_1^0$ mass plane. The SR with the best expected sensitivity is adopted for each point of the parameter space. The yellow band around the expected limit (dashed line) shows the impact of the experimental and SM background theoretical uncertainties. The dotted lines show the impact on the observed limit of the variation of the nominal signal cross-section by $\pm 1\sigma$ of its theoretical uncertainties. The exclusion limits from the Run-1 ATLAS searches [72,81] and from the 13 TeV monojet search [82] are also superimposed. The latter limit is only published for values of $m_{\tilde{b}_1} - m_{\tilde{\chi}_1^0} = 5$ and 20 GeV

Furthermore, the sensitivity of the analysis benefits from the advanced algorithms adopted to identify b -jets and use of information from the newly installed IBL pixel layer in the Run-2 ATLAS detector, as well as from improved techniques to estimate SM background contributions and their systematic uncertainties.

9 Conclusion

In summary, the results of a search for bottom squark pair production are reported. The analysis uses 3.2 fb^{-1} of pp collisions at $\sqrt{s} = 13 \text{ TeV}$ collected by the ATLAS experi-

ment at the Large Hadron Collider in 2015. Bottom squarks are searched for in events containing large missing transverse momentum and up to four jets, exactly two of which are identified as b -jets. No excess above the expected Standard Model background yield is found. Exclusion limits at 95 % confidence level are placed on the visible cross-section and on the mass of the bottom squark in phenomenological supersymmetric R -parity-conserving models in which the \tilde{b}_1 is the lightest squark and is assumed to decay exclusively via $\tilde{b}_1 \rightarrow b\tilde{\chi}_1^0$, where $\tilde{\chi}_1^0$ is the lightest neutralino. Bottom squark masses up to 800 GeV are excluded for $\tilde{\chi}_1^0$ masses below 360 GeV (840 GeV for $\tilde{\chi}_1^0$ masses below 100 GeV) whilst differences in mass above 100 GeV between \tilde{b}_1 and $\tilde{\chi}_1^0$ are excluded up to \tilde{b}_1 masses of 500 GeV. The results significantly extend the constraints on bottom squark masses with respect to Run-1 searches.

Acknowledgments We thank CERN for the very successful operation of the LHC, as well as the support staff from our institutions without whom ATLAS could not be operated efficiently. We acknowledge the support of ANPCyT, Argentina; YerPhI, Armenia; ARC, Australia; BMWFW and FWF, Austria; ANAS, Azerbaijan; SSTC, Belarus; CNPq and FAPESP, Brazil; NSERC, NRC and CFI, Canada; CERN; CONICYT, Chile; CAS, MOST and NSFC, China; COLCIENCIAS, Colombia; MSMT CR, MPO CR and VSC CR, Czech Republic; DNRF and DNSRC, Denmark; IN2P3-CNRS, CEA-DSM/IRFU, France; GNSF, Georgia; BMBF, HGF, and MPG, Germany; GSRT, Greece; RGC, Hong Kong SAR, China; ISF, I-CORE and Benoziyo Center, Israel; INFN, Italy; MEXT and JSPS, Japan; CNRST, Morocco; FOM and NWO, Netherlands; RCN, Norway; MNiSW and NCN, Poland; FCT, Portugal; MNE/IFA, Romania; MES of Russia and NRC KI, Russian Federation; JINR; MESTD, Serbia; MSSR, Slovakia; ARRS and MIZŠ, Slovenia; DST/NRF, South Africa; MINECO, Spain; SRC and Wallenberg Foundation, Sweden; SERI, SNSF and Cantons of Bern and Geneva, Switzerland; MOST, Taiwan; TAEK, Turkey; STFC, United Kingdom; DOE and NSF, United States of America. In addition, individual groups and members have received support from BCKDF, the Canada Council, CANARIE, CRC, Compute Canada, FQRNT, and the Ontario Innovation Trust, Canada; EPLANET, ERC, FP7, Horizon 2020 and Marie Skłodowska-Curie Actions, European Union; Investissements d'Avenir Labex and Idex, ANR, Région Auvergne and Fondation Partager le Savoir, France; DFG and AvH Foundation, Germany; Herakleitos, Thales and Aristeia programmes co-financed by EU-ESF and the Greek NSRF; BSF, GIF and Minerva, Israel; BRF, Norway; Generalitat de Catalunya, Generalitat Valenciana, Spain; the Royal Society and Leverhulme Trust, United Kingdom. The crucial computing support from all WLCG partners is acknowledged gratefully, in particular from CERN, the ATLAS Tier-1 facilities at TRIUMF (Canada), NDGF (Denmark, Norway, Sweden), CC-IN2P3 (France), KIT/GridKA (Germany), INFN-CNAF (Italy), NL-T1 (Netherlands), PIC (Spain), ASGC (Taiwan), RAL (UK) and BNL (USA), the Tier-2 facilities worldwide and large non-WLCG resource providers. Major contributors of computing resources are listed in Ref. [83].

Open Access This article is distributed under the terms of the Creative Commons Attribution 4.0 International License (<http://creativecommons.org/licenses/by/4.0/>), which permits unrestricted use, distribution, and reproduction in any medium, provided you give appropriate credit to the original author(s) and the source, provide a link to the Creative Commons license, and indicate if changes were made. Funded by SCOAP³.

References

1. Y.A. Gol'fand, E.P. Likhtman, JETP Lett. **13**, 323–326 (1971). [Pisma Zh. Eksp. Teor. Fiz. 13 (1971) 452]
2. D.V. Volkov, V.P. Akulov, Phys. Lett. B **46**, 109 (1973)
3. J. Wess, B. Zumino, Nucl. Phys. B **70**, 39 (1974)
4. J. Wess, B. Zumino, Nucl. Phys. B **78**, 1 (1974)
5. S. Ferrara, B. Zumino, Nucl. Phys. B **79**, 413 (1974)
6. A. Salam, J.A. Strathdee, Phys. Lett. B **51**, 353 (1974)
7. N. Sakai, Z. Phys. C **11**, 153 (1981)
8. S. Dimopoulos, S. Raby, F. Wilczek, Phys. Rev. D **24**, 1681 (1981)
9. L.E. Ibanez, G.G. Ross, Phys. Lett. B **105**, 439 (1981)
10. S. Dimopoulos, H. Georgi, Nucl. Phys. B **193**, 150 (1981)
11. P. Fayet, Phys. Lett. B **64**, 159 (1976)
12. P. Fayet, Phys. Lett. B **69**, 489 (1977)
13. G.R. Farrar, P. Fayet, Phys. Lett. B **76**, 575 (1978)
14. H. Goldberg, Phys. Rev. Lett. **50**, 1419 (1983). [Erratum: Phys. Rev. Lett. **103** (2009) 099905]
15. J.R. Ellis, J.S. Hagelin, D.V. Nanopoulos, K.A. Olive, M. Srednicki, Nucl. Phys. B **238**, 453 (1984)
16. R. Barbieri, G.F. Giudice, Nucl. Phys. B **306**, 63 (1988)
17. B. de Carlos, J.A. Casas, Phys. Lett. B **309**, 320 (1993). [arXiv:hep-ph/9303291](https://arxiv.org/abs/hep-ph/9303291)
18. ATLAS Collaboration, JHEP **1510**, 134 (2015). [arXiv:1508.06608](https://arxiv.org/abs/1508.06608) [hep-ex]
19. ATLAS Collaboration, Eur. Phys. J. C **75**, 510 (2015). [arXiv:1506.08616](https://arxiv.org/abs/1506.08616) [hep-ex]
20. CMS Collaboration, JHEP **1506**, 116 (2015). [arXiv:1503.08037](https://arxiv.org/abs/1503.08037) [hep-ex]
21. ATLAS Collaboration, JINST **3**, S08003 (2008)
22. ATLAS Collaboration, ATLAS-TDR-19 (2010). <http://cds.cern.ch/record/1291633>. Addendum: ATLAS-TDR-19-ADD-1 (2012). <http://cds.cern.ch/record/1451888>
23. ATLAS Collaboration, Eur. Phys. J. C **72**, 1849 (2012). [arXiv:1110.1530](https://arxiv.org/abs/1110.1530) [hep-ex]
24. ATLAS Collaboration, Eur. Phys. J. C **73**, 2518 (2013). [arXiv:1302.4393](https://arxiv.org/abs/1302.4393) [hep-ex]
25. ATLAS Collaboration, Eur. Phys. J. C **70**, 823 (2010). [arXiv:1005.4568](https://arxiv.org/abs/1005.4568) [hep-ex]
26. S. Agostinelli et al. (GEANT4), Nucl. Instrum. Methods A **506**, 250 (2003)
27. ATLAS Collaboration, ATL-PHYS-PUB-2010-013 (2010). <http://cds.cern.ch/record/1300517>
28. T. Sjostrand, S. Mrenna, P.Z. Skands, Comput. Phys. Commun. **178**, 852 (2008). [arXiv:0710.3820](https://arxiv.org/abs/0710.3820) [hep-ph]
29. A.D. Martin, W.J. Stirling, R.S. Thorne, G. Watt, Eur. Phys. J. C **63**, 189 (2009). [arXiv:0901.0002](https://arxiv.org/abs/0901.0002) [hep-ph]
30. A. Martin, W. Stirling, R. Thorne, G. Watt, Phys. Lett. B **652**, 292 (2007). [arXiv:0706.0459](https://arxiv.org/abs/0706.0459) [hep-ph]
31. J. Alwall et al., JHEP **1407**, 079 (2014). [arXiv:1405.0301](https://arxiv.org/abs/1405.0301) [hep-ph]
32. ATLAS Collaboration, ATL-PHYS-PUB-2014-021 (2014). <http://cdsweb.cern.ch/record/1966419>
33. R.D. Ball et al., Nucl. Phys. B **867**, 244 (2013). [arXiv:1207.1303](https://arxiv.org/abs/1207.1303) [hep-ph]
34. L. Lönnblad, S. Prestel, JHEP **1303**, 166 (2013). [arXiv:1211.7278](https://arxiv.org/abs/1211.7278) [hep-ph]
35. W. Beenakker, M. Kramer, T. Plehn, M. Spira, P.M. Zerwas, Nucl. Phys. B **515**, 3 (1998). [arXiv:hep-ph/9710451](https://arxiv.org/abs/hep-ph/9710451)
36. W. Beenakker et al., JHEP **1008**, 098 (2010). [arXiv:1006.4771](https://arxiv.org/abs/1006.4771) [hep-ph]
37. W. Beenakker et al., Int. J. Mod. Phys. A **26**, 2637 (2011). [arXiv:1105.1110](https://arxiv.org/abs/1105.1110) [hep-ph]
38. T. Gleisberg et al., JHEP **0902**, 007 (2009). [arXiv:0811.4622](https://arxiv.org/abs/0811.4622) [hep-ph]
39. T. Gleisberg, S. Höche, JHEP **0812**, 039 (2008). [arXiv:0808.3674](https://arxiv.org/abs/0808.3674) [hep-ph]
40. F. Cascioli, P. Maierhofer, S. Pozzorini, Phys. Rev. Lett. **108**, 111601 (2012). [arXiv:1111.5206](https://arxiv.org/abs/1111.5206) [hep-ph]
41. S. Schumann, F. Krauss, JHEP **0803**, 038 (2008). [arXiv:0709.1027](https://arxiv.org/abs/0709.1027) [hep-ph]
42. S. Höche, F. Krauss, M. Schönherr, F. Siegert, JHEP **1304**, 027 (2013). [arXiv:1207.5030](https://arxiv.org/abs/1207.5030) [hep-ph]
43. H.-L. Lai et al., Phys. Rev. D **82**, 074024 (2010). [arXiv:1007.2241](https://arxiv.org/abs/1007.2241) [hep-ph]
44. R. Gavin, Y. Li, F. Petriello, S. Quackenbush, Comput. Phys. Commun. **182**, 2388 (2011). [arXiv:1011.3540](https://arxiv.org/abs/1011.3540) [hep-ph]
45. K.A. Olive et al. (Particle Data Group), Chin. Phys. C **38**, 090001 (2015)
46. S. Alioli, P. Nason, C. Oleari, E. Re, JHEP **1006**, 043 (2010). [arXiv:1002.2581](https://arxiv.org/abs/1002.2581) [hep-ph]
47. ATLAS Collaboration, ATL-PHYS-PUB-2016-004 (2016). <http://cdsweb.cern.ch/record/2120417>
48. T. Sjostrand, S. Mrenna, P.Z. Skands, JHEP **0605**, 026 (2006). [arXiv:hep-ph/0603175](https://arxiv.org/abs/hep-ph/0603175)
49. P.Z. Skands, Phys. Rev. D **82**, 074018 (2010). [arXiv:1005.3457](https://arxiv.org/abs/1005.3457) [hep-ph]
50. M. Czakon, A. Mitov, Comput. Phys. Commun. **185**, 2930 (2014). [arXiv:1112.5675](https://arxiv.org/abs/1112.5675) [hep-ph]
51. N. Kidonakis, Phys. Rev. D **83**, 091503 (2011). [arXiv:1103.2792](https://arxiv.org/abs/1103.2792) [hep-ph]
52. N. Kidonakis, Phys. Rev. D **81**, 054028 (2010). [arXiv:1001.5034](https://arxiv.org/abs/1001.5034) [hep-ph]
53. N. Kidonakis, Phys. Rev. D **82**, 054018 (2010). [arXiv:1005.4451](https://arxiv.org/abs/1005.4451) [hep-ph]
54. D.J. Lange, Nucl. Instrum. Methods A **462**, 152 (2001)
55. ATLAS Collaboration, ATL-PHYS-PUB-2015-026 (2015). <http://cdsweb.cern.ch/record/2037717>
56. ATLAS Collaboration, [arXiv:1603.02934](https://arxiv.org/abs/1603.02934) [hep-ex] (submitted to Eur. Phys. J. C)
57. M. Cacciari, G.P. Salam, G. Soyez, JHEP **0804**, 063 (2008). [arXiv:0802.1189](https://arxiv.org/abs/0802.1189) [hep-ph]
58. ATLAS Collaboration, ATL-PHYS-PUB-2015-015 (2015). <http://cds.cern.ch/record/2037613>
59. ATLAS Collaboration, ATLAS-CONF-2015-037 (2015). <http://cdsweb.cern.ch/record/2044941>
60. ATLAS Collaboration, ATLAS-CONF-2015-029 (2015). <http://cdsweb.cern.ch/record/2037702>
61. ATLAS Collaboration, ATLAS-CONF-2014-018 (2014). <http://cdsweb.cern.ch/record/1700870>
62. ATLAS Collaboration, ATL-PHYS-PUB-2015-039 (2015). <http://cdsweb.cern.ch/record/2047871>
63. ATLAS Collaboration, ATLAS-CONF-2014-046 (2014). <http://cdsweb.cern.ch/record/1741020>
64. ATLAS Collaboration, JINST **11**, P04008 (2016). [arXiv:1512.01094](https://arxiv.org/abs/1512.01094) [hep-ex]
65. ATLAS Collaboration, Eur. Phys. J. C **74**, 2941 (2014). [arXiv:1404.2240](https://arxiv.org/abs/1404.2240) [hep-ex]
66. ATLAS Collaboration, Eur. Phys. J. C **74**, 3071 (2014). [arXiv:1407.5063](https://arxiv.org/abs/1407.5063) [hep-ex]
67. ATLAS Collaboration, ATL-PHYS-PUB-2015-041 (2015). <http://cdsweb.cern.ch/record/2048202>
68. ATLAS Collaboration, [arXiv:1603.05598](https://arxiv.org/abs/1603.05598) [hep-ex] (submitted to Eur. Phys. J. C)
69. ATLAS Collaboration, ATLAS-CONF-2013-082 (2013). <http://cdsweb.cern.ch/record/1570993>
70. ATLAS Collaboration, Eur. Phys. J. C **73**, 2304 (2013). [arXiv:1112.6426](https://arxiv.org/abs/1112.6426) [hep-ex]
71. ATLAS Collaboration, ATLAS-CONF-2012-123 (2012). <http://cdsweb.cern.ch/record/1473426>

72. ATLAS Collaboration, JHEP **1310**, 189 (2013). [arXiv:1308.2631](#) [hep-ex]
73. D.R. Tovey, JHEP **0804**, 034 (2008). [arXiv:0802.2879](#) [hep-ph]
74. M. Baak et al., Eur. Phys. J. C **75**, 153 (2015). [arXiv:1410.1280](#) [hep-ex]
75. G. Cowan, K. Cranmer, E. Gross, O. Vitells, Eur. Phys. J. C **71**, 1554 (2011). [arXiv:1007.1727](#) [physics.data-an]. [Erratum: Eur. Phys. J. C **73** (2013) 2501]
76. ATLAS Collaboration, Phys. Rev. D **87**, 012008 (2013). [arXiv:1208.0949](#) [hep-ex]
77. ATLAS Collaboration, Phys. Lett. B **707**, 418 (2012). [arXiv:1109.1470](#) [hep-ex]
78. M. Bähr et al., Eur. Phys. J. C **58**, 639 (2008). [arXiv:0803.0883](#) [hep-ph]
79. T. Junk, Nucl. Instrum. Methods A **434**, 435 (1999). [arXiv:hep-ex/9902006](#)
80. A.L. Read, J. Phys. G **28**, 2693 (2002)
81. ATLAS Collaboration, Phys. Rev. D **90**, 052008 (2014). [arXiv:1407.0608](#) [hep-ex]
82. ATLAS Collaboration, [arXiv:1604.07773](#) [hep-ex] (submitted to Phys. Rev. D)
83. ATLAS Collaboration, ATL-GEN-PUB-2016-002 (2016). <http://cds.cern.ch/record/2202407>

ATLAS Collaboration

M. Aaboud^{135d}, G. Aad⁸⁶, B. Abbott¹¹³, J. Abdallah⁶⁴, O. Abidinov¹², B. Abeloos¹¹⁷, R. Aben¹⁰⁷, O. S. AbouZeid¹³⁷, N. L. Abraham¹⁴⁹, H. Abramowicz¹⁵³, H. Abreu¹⁵², R. Abreu¹¹⁶, Y. Abulaiti^{146a,146b}, B. S. Acharya^{163a,163b,a}, L. Adamczyk^{40a}, D. L. Adams²⁷, J. Adelman¹⁰⁸, S. Adomeit¹⁰⁰, T. Adye¹³¹, A. A. Affolder⁷⁵, T. Agatonovic-Jovin¹⁴, J. Agricola⁵⁶, J. A. Aguilar-Saavedra^{126a,126f}, S. P. Ahlen²⁴, F. Ahmadov^{66,b}, G. Aielli^{133a,133b}, H. Akerstedt^{146a,146b}, T. P. A. Åkesson⁸², A. V. Akimov⁹⁶, G. L. Alberghi^{22a,22b}, J. Albert¹⁶⁸, S. Albrand⁵⁷, M. J. Alconada Verzini⁷², M. Aleksa³², I. N. Aleksandrov⁶⁶, C. Alexa^{28b}, G. Alexander¹⁵³, T. Alexopoulos¹⁰, M. Alhroob¹¹³, B. Ali¹²⁸, M. Aliev^{74a,74b}, G. Alimonti^{92a}, J. Alison³³, S. P. Alkire³⁷, B. M. M. Allbrooke¹⁴⁹, B. W. Allen¹¹⁶, P. P. Allport¹⁹, A. Aloisio^{104a,104b}, A. Alonso³⁸, F. Alonso⁷², C. Alpigiani¹³⁸, M. Alstady⁸⁶, B. Alvarez Gonzalez³², D. Álvarez Piqueras¹⁶⁶, M. G. Alvigi^{104a,104b}, B. T. Amadio¹⁶, K. Amako⁶⁷, Y. Amaral Coutinho^{26a}, C. Amelung²⁵, D. Amidei⁹⁰, S. P. Amor Dos Santos^{126a,126c}, A. Amorim^{126a,126b}, S. Amoroso³², G. Amundsen²⁵, C. Anastopoulos¹³⁹, L. S. Ancu⁵¹, N. Andari¹⁹, T. Andeen¹¹, C. F. Anders^{59b}, G. Anders³², J. K. Anders⁷⁵, K. J. Anderson³³, A. Andreazza^{92a,92b}, V. Andrei^{59a}, S. Angelidakis⁹, I. Angelozzi¹⁰⁷, P. Anger⁴⁶, A. Angerami³⁷, F. Anghinolfi³², A. V. Anisenkov^{109,c}, N. Anjos¹³, A. Annovi^{124a,124b}, C. Antel^{59a}, M. Antonelli⁴⁹, A. Antonov^{98,*}, F. Anulli^{132a}, M. Aoki⁶⁷, L. Aperio Bella¹⁹, G. Arabidze⁹¹, Y. Arai⁶⁷, J. P. Araque^{126a}, A. T. H. Arce⁴⁷, F. A. Arduh⁷², J.-F. Arguin⁹⁵, S. Argyropoulos⁶⁴, M. Arik^{20a}, A. J. Armbruster¹⁴³, L. J. Armitage⁷⁷, O. Arnaez³², H. Arnold⁵⁰, M. Arratia³⁰, O. Arslan²³, A. Artamonov⁹⁷, G. Artoni¹²⁰, S. Artz⁸⁴, S. Asai¹⁵⁵, N. Asbah⁴⁴, A. Ashkenazi¹⁵³, B. Åsman^{146a,146b}, L. Asquith¹⁴⁹, K. Assamagan²⁷, R. Astalos^{144a}, M. Atkinson¹⁶⁵, N. B. Atlay¹⁴¹, K. Augsten¹²⁸, G. Avolio³², B. Axen¹⁶, M. K. Ayoub¹¹⁷, G. Azuelos^{95,d}, M. A. Baak³², A. E. Baas^{59a}, M. J. Baca¹⁹, H. Bachacou¹³⁶, K. Bachas^{74a,74b}, M. Backes¹⁴⁸, M. Backhaus³², P. Bagiacchi^{132a,132b}, P. Bagnaia^{132a,132b}, Y. Bai^{35a}, J. T. Baines¹³¹, O. K. Baker¹⁷⁵, E. M. Baldin^{109,c}, P. Balek¹⁷¹, T. Balestri¹⁴⁸, F. Balli¹³⁶, W. K. Balunas¹²², E. Banas⁴¹, Sw. Banerjee^{172,e}, A. A. E. Bannoura¹⁷⁴, L. Barak³², E. L. Barberio⁸⁹, D. Barberis^{52a,52b}, M. Barbero⁸⁶, T. Barillari¹⁰¹, M.-S. Barisits³², T. Barklow¹⁴³, N. Barlow³⁰, S. L. Barnes⁸⁵, B. M. Barnett¹³¹, R. M. Barnett¹⁶, Z. Barnovska⁵, A. Baroncelli^{134a}, G. Barone²⁵, A. J. Barr¹²⁰, L. Barranco Navarro¹⁶⁶, F. Barreiro⁸³, J. Barreiro Guimarães da Costa^{35a}, R. Bartoldus¹⁴³, A. E. Barton⁷³, P. Bartos^{144a}, A. Basalae¹²³, A. Bassalat¹¹⁷, R. L. Bates⁵⁵, S. J. Batista¹⁵⁸, J. R. Batley³⁰, M. Battaglia¹³⁷, M. Bause^{132a,132b}, F. Bauer¹³⁶, H. S. Bawa^{143,f}, J. B. Beacham¹¹¹, M. D. Beattie⁷³, T. Beau⁸¹, P. H. Beauchemin¹⁶¹, P. Bechtel²³, H. P. Beck^{18,g}, K. Becker¹²⁰, M. Becker⁸⁴, M. Beckingham¹⁶⁹, C. Becot¹¹⁰, A. J. Beddall^{20d}, A. Beddall^{20b}, V. A. Bednyakov⁶⁶, M. Bedognetti¹⁰⁷, C. P. Bee¹⁴⁸, L. J. Beemster¹⁰⁷, T. A. Beermann³², M. Begel²⁷, J. K. Behr⁴⁴, C. Belanger-Champagne⁸⁸, A. S. Bell⁷⁹, G. Bella¹⁵³, L. Bellagamba^{22a}, A. Bellerive³¹, M. Bellomo⁸⁷, K. Belotskiy⁹⁸, O. Beltramello³², N. L. Belyaev⁹⁸, O. Benary¹⁵³, D. Bencheikroun^{135a}, M. Bender¹⁰⁰, K. Bendtz^{146a,146b}, N. Benekos¹⁰, Y. Benhammou¹⁵³, E. Benhar Nocchioli¹⁷⁵, J. Benítez⁶⁴, D. P. Benjamin⁴⁷, J. R. Bensinger²⁵, S. Bentvelsen¹⁰⁷, L. Beresford¹²⁰, M. Beretta⁴⁹, D. Berge¹⁰⁷, E. Bergeas Kuutmann¹⁶⁴, N. Berger⁵, J. Beringer¹⁶, S. Berlendis⁵⁷, N. R. Bernard⁸⁷, C. Bernius¹¹⁰, F. U. Bernlochner²³, T. Berry⁷⁸, P. Berta¹²⁹, C. Bertella⁸⁴, G. Bertoli^{146a,146b}, F. Bertolucci^{124a,124b}, I. A. Bertram⁷³, C. Bertsche⁴⁴, D. Bertsche¹¹³, G. J. Besjes³⁸, O. Bessidskaia Bylund^{146a,146b}, M. Bessner⁴⁴, N. Besson¹³⁶, C. Betancourt⁵⁰, A. Bethani⁵⁷, S. Bethke¹⁰¹, A. J. Bevan⁷⁷, R. M. Bianchi¹²⁵, L. Bianchini²⁵, M. Bianco³², O. Biebel¹⁰⁰, D. Biedermann¹⁷, R. Bielski⁸⁵, N. V. Biesuz^{124a,124b}, M. Biglietti^{134a}, J. Bilbao De Mendizabal⁵¹, T. R. V. Billoud⁹⁵, H. Bilokon⁴⁹, M. Bindi⁵⁶, S. Binet¹¹⁷, A. Bingul^{20b}, C. Bini^{132a,132b}, S. Biondi^{22a,22b}, T. Bisanz⁵⁶, D. M. Bjergaard⁴⁷, C. W. Black¹⁵⁰, J. E. Black¹⁴³, K. M. Black²⁴, D. Blackburn¹³⁸, R. E. Blair⁶, J.-B. Blanchard¹³⁶, T. Blazek^{144a}, I. Bloch⁴⁴, C. Blocker²⁵, W. Blum^{84,*}, U. Blumenschein⁵⁶, S. Blunier^{34a}, G. J. Bobbink¹⁰⁷, V. S. Bobrovnikov^{109,c}, S. S. Bocchetta⁸², A. Bocci⁴⁷, C. Bock¹⁰⁰, M. Boehler⁵⁰, D. Boerner¹⁷⁴, J. A. Bogaerts³², D. Bogavac¹⁴, A. G. Bogdanchikov¹⁰⁹, C. Bohm^{146a}, V. Boisvert⁷⁸,

- P. Bokan¹⁴, T. Bold^{40a}, A. S. Boldyrev^{163a,163c}, M. Bomben⁸¹, M. Bona⁷⁷, M. Boonekamp¹³⁶, A. Borisov¹³⁰, G. Borissov⁷³, J. Bortfeldt³², D. Bortoletto¹²⁰, V. Bortolotto^{61a,61b,61c}, K. Bos¹⁰⁷, D. Boscherini^{22a}, M. Bosman¹³, J. D. Bossio Sola²⁹, J. Boudreau¹²⁵, J. Bouffard², E. V. Bouhova-Thacker⁷³, D. Boumediene³⁶, C. Bourdarios¹¹⁷, S. K. Boutle⁵⁵, A. Boveia³², J. Boyd³², I. R. Boyko⁶⁶, J. Bracinik¹⁹, A. Brandt⁸, G. Brandt⁵⁶, O. Brandt^{59a}, U. Bratzler¹⁵⁶, B. Brau⁸⁷, J. E. Brau¹¹⁶, H. M. Braun^{174,*}, W. D. Breaden Madden⁵⁵, K. Brendlinger¹²², A. J. Brennan⁸⁹, L. Brenner¹⁰⁷, R. Brenner¹⁶⁴, S. Bressler¹⁷¹, T. M. Bristow⁴⁸, D. Britton⁵⁵, D. Britzger⁴⁴, F. M. Brochu³⁰, I. Brock²³, R. Brock⁹¹, G. Brooijmans³⁷, T. Brooks⁷⁸, W. K. Brooks^{34b}, J. Brosamer¹⁶, E. Brost¹⁰⁸, J. H. Broughton¹⁹, P. A. Bruckman de Renstrom⁴¹, D. Bruncko^{144b}, R. Bruneliere⁵⁰, A. Bruni^{22a}, G. Bruni^{22a}, L. S. Bruni¹⁰⁷, B. H. Brunt³⁰, M. Bruschi^{22a}, N. Bruscino²³, P. Bryant³³, L. Bryngemark⁸², T. Buanes¹⁵, Q. Buat¹⁴², P. Buchholz¹⁴¹, A. G. Buckley⁵⁵, I. A. Budagov⁶⁶, F. Buehrer⁵⁰, M. K. Bugge¹¹⁹, O. Bulekov⁹⁸, D. Bullock⁸, H. Burckhart³², S. Burdin⁷⁵, C. D. Burgard⁵⁰, B. Burghgrave¹⁰⁸, K. Burka⁴¹, S. Burke¹³¹, I. Burmeister⁴⁵, J. T. P. Burr¹²⁰, E. Busato³⁶, D. Büscher⁵⁰, V. Büscher⁸⁴, P. Bussey⁵⁵, J. M. Butler²⁴, C. M. Buttar⁵⁵, J. M. Butterworth⁷⁹, P. Butti¹⁰⁷, W. Buttinger²⁷, A. Buzatu⁵⁵, A. R. Buzykaev^{109,c}, S. Cabrera Urbán¹⁶⁶, D. Caforio¹²⁸, V. M. Cairo^{39a,39b}, O. Cakir^{4a}, N. Calace⁵¹, P. Calafiura¹⁶, A. Calandri⁸⁶, G. Calderini⁸¹, P. Calfayan¹⁰⁰, G. Callea^{39a,39b}, L. P. Caloba^{26a}, S. Calvente Lopez⁸³, D. Calvet³⁶, S. Calvet³⁶, T. P. Calvet⁸⁶, R. Camacho Toro³³, S. Camarda³², P. Camarri^{133a,133b}, D. Cameron¹¹⁹, R. Caminal Armadans¹⁶⁵, C. Camincher⁵⁷, S. Campana³², M. Campanelli⁷⁹, A. Camplani^{92a,92b}, A. Campoverde¹⁴¹, V. Canale^{104a,104b}, A. Canepa^{159a}, M. Cano Bret^{35e}, J. Cantero¹¹⁴, R. Cantrill^{126a}, T. Cao⁴², M. D. M. Capeans Garrido³², I. Caprini^{28b}, M. Caprini^{28b}, M. Capua^{39a,39b}, R. Caputo⁸⁴, R. M. Carbone³⁷, R. Cardarelli^{133a}, F. Cardillo⁵⁰, I. Carli¹²⁹, T. Carli³², G. Carlino^{104a}, L. Carminati^{92a,92b}, S. Caron¹⁰⁶, E. Carquin^{34b}, G. D. Carrillo-Montoya³², J. R. Carter³⁰, J. Carvalho^{126a,126c}, D. Casadei¹⁹, M. P. Casado^{13,h}, M. Casolino¹³, D. W. Casper¹⁶², E. Castaneda-Miranda^{145a}, R. Castelijin¹⁰⁷, A. Castelli¹⁰⁷, V. Castillo Gimenez¹⁶⁶, N. F. Castro^{126a,i}, A. Catinaccio³², J. R. Catmore¹¹⁹, A. Cattai³², J. Caudron²³, V. Cavaliere¹⁶⁵, E. Cavallaro¹³, D. Cavalli^{92a}, M. Cavalli-Sforza¹³, V. Cavasinni^{124a,124b}, F. Ceradini^{134a,134b}, L. Cerda Alberich¹⁶⁶, B. C. Cerio⁴⁷, A. S. Cerqueira^{26b}, A. Cerri¹⁴⁹, L. Cerrito^{133a,133b}, F. Cerutti¹⁶, M. Cerv³², A. Cervelli¹⁸, S. A. Cetin^{20c}, A. Chafaq^{135a}, D. Chakraborty¹⁰⁸, S. K. Chan⁵⁸, Y. L. Chan^{61a}, P. Chang¹⁶⁵, J. D. Chapman³⁰, D. G. Charlton¹⁹, A. Chatterjee⁵¹, C. C. Chau¹⁵⁸, C. A. Chavez Barajas¹⁴⁹, S. Che¹¹¹, S. Cheatham⁷³, A. Chegwidan⁹¹, S. Chekanov⁶, S. V. Chekulaev^{159a}, G. A. Chelkov^{66j}, M. A. Chelstowska⁹⁰, C. Chen⁶⁵, H. Chen²⁷, K. Chen¹⁴⁸, S. Chen^{35c}, S. Chen¹⁵⁵, X. Chen^{35f}, Y. Chen⁶⁸, H. C. Cheng⁹⁰, H. J. Cheng^{35a}, Y. Cheng³³, A. Cheplakov⁶⁶, E. Cheremushkina¹³⁰, R. Cherkaoui El Moursli^{135e}, V. Chernyatin^{27,*}, E. Cheu⁷, L. Chevalier¹³⁶, V. Chiarella⁴⁹, G. Chiarelli^{124a,124b}, G. Chiodini^{74a}, A. S. Chisholm¹⁹, A. Chitan^{28b}, M. V. Chizhov⁶⁶, K. Choi⁶², A. R. Chomont³⁶, S. Chouridou⁹, B. K. B. Chow¹⁰⁰, V. Christodoulou⁷⁹, D. Chromek-Burckhart³², J. Chudoba¹²⁷, A. J. Chuinard⁸⁸, J. J. Chwastowski⁴¹, L. Chytka¹¹⁵, G. Ciapetti^{132a,132b}, A. K. Ciftci^{4a}, D. Cinca⁴⁵, V. Cindro⁷⁶, I. A. Cioara²³, C. Ciocca^{22a,22b}, A. Ciochio¹⁶, F. Ciotto^{104a,104b}, Z. H. Citron¹⁷¹, M. Citterio^{92a}, M. Ciubancan^{28b}, A. Clark⁵¹, B. L. Clark⁵⁸, M. R. Clark³⁷, P. J. Clark⁴⁸, R. N. Clarke¹⁶, C. Clement^{146a,146b}, Y. Coadou⁸⁶, M. Cobl^{163a,163c}, A. Coccaro⁵¹, J. Cochran⁶⁵, L. Colasurdo¹⁰⁶, B. Cole³⁷, A. P. Colijn¹⁰⁷, J. Collot⁵⁷, T. Colombo³², G. Compostella¹⁰¹, P. Conde Muino^{126a,126b}, E. Coniavitis⁵⁰, S. H. Connell^{145b}, I. A. Connelly⁷⁸, V. Consorti⁵⁰, S. Constantinescu^{28b}, G. Conti³², F. Conventi^{104a,k}, M. Cooke¹⁶, B. D. Cooper⁷⁹, A. M. Cooper-Sarkar¹²⁰, K. J. R. Cormier¹⁵⁸, T. Cornelissen¹⁷⁴, M. Corradi^{132a,132b}, F. Corriveau^{88,1}, A. Corso-Radu¹⁶², A. Cortes-Gonzalez³², G. Cortiana¹⁰¹, G. Costa^{92a}, M. J. Costa¹⁶⁶, D. Costanzo¹³⁹, G. Cottin³⁰, G. Cowan⁷⁸, B. E. Cox⁸⁵, K. Cranmer¹¹⁰, S. J. Crawley⁵⁵, G. Cree³¹, S. Crépe-Renaudin⁵⁷, F. Crescioli⁸¹, W. A. Cribbs^{146a,146b}, M. Crispin Ortuzar¹²⁰, M. Cristinziani²³, V. Croft¹⁰⁶, G. Crosetti^{39a,39b}, A. Cueto⁸³, T. Cuhadar Donszelmann¹³⁹, J. Cummings¹⁷⁵, M. Curatolo⁴⁹, J. Cúth⁸⁴, H. Czini¹⁴¹, P. Czodrowski³, G. D'amen^{22a,22b}, S. D'Auria⁵⁵, M. D'Onofrio⁷⁵, M. J. Da Cunha Sargedas De Sousa^{126a,126b}, C. Da Via⁸⁵, W. Dabrowski^{40a}, T. Dado^{144a}, T. Dai⁹⁰, O. Dale¹⁵, F. Dallahire⁹⁵, C. Dallapiccola⁸⁷, M. Dam³⁸, J. R. Dandoy³³, N. P. Dang⁵⁰, A. C. Daniells¹⁹, N. S. Dann⁸⁵, M. Danninger¹⁶⁷, M. Dano Hoffmann¹³⁶, V. Dao⁵⁰, G. Darbo^{52a}, S. Darmora⁸, J. Dassoulas³, A. Dattagupta⁶², W. Davey²³, C. David¹⁶⁸, T. Davidek¹²⁹, M. Davies¹⁵³, P. Davison⁷⁹, E. Dawe⁸⁹, I. Dawson¹³⁹, R. K. Daya-Ishmukhametova⁸⁷, K. De⁸, R. de Asmundis^{104a}, A. De Benedetti¹¹³, S. De Castro^{22a,22b}, S. De Cecco⁸¹, N. De Groot¹⁰⁶, P. de Jong¹⁰⁷, H. De la Torre⁸³, F. De Lorenzi⁶⁵, A. De Maria⁵⁶, D. De Pedis^{132a}, A. De Salvo^{132a}, U. De Sanctis¹⁴⁹, A. De Santo¹⁴⁹, J. B. De Vivie De Regie¹¹⁷, W. J. Dearnaley⁷³, R. Debbi²⁷, C. Debenedetti¹³⁷, D. V. Dedovich⁶⁶, N. Dehghanian³, I. Deigaard¹⁰⁷, M. Del Gaudio^{39a,39b}, J. Del Peso⁸³, T. Del Prete^{124a,124b}, D. Delgove¹¹⁷, F. Deliot¹³⁶, C. M. Delitzsch⁵¹, A. Dell'Acqua³², L. Dell'Asta²⁴, M. Dell'Orso^{124a,124b}, M. Della Pietra^{104a,k}, D. della Volpe⁵¹, M. Delmastro⁵, P. A. Delsart⁵⁷, D. A. DeMarco¹⁵⁸, S. Demers¹⁷⁵, M. Demichev⁶⁶, A. Demilly⁸¹, S. P. Denisov¹³⁰, D. Denysiuk¹³⁶, D. Derendarz⁴¹, J. E. Derkaoui^{135d}, F. Derue⁸¹, P. Dervan⁷⁵, K. Desch²³, C. Deterre⁴⁴, K. Dette⁴⁵, P. O. Deviveiros³², A. Dewhurst¹³¹, S. Dhaliwal²⁵, A. Di Ciaccio^{133a,133b}, L. Di Ciaccio⁵, W. K. Di Clemente¹²², C. Di Donato^{132a,132b}, A. Di Girolamo³², B. Di Girolamo³², B. Di Micco^{134a,134b}, R. Di Nardo³², A. Di Simone⁵⁰, R. Di Sipio¹⁵⁸,

D. Di Valentino³¹, C. Diaconu⁸⁶, M. Diamond¹⁵⁸, F. A. Dias⁴⁸, M. A. Diaz^{34a}, E. B. Diehl⁹⁰, J. Dietrich¹⁷, S. Diglio⁸⁶, A. Dimitrievska¹⁴, J. Dingfelder²³, P. Dita^{28b}, S. Dita^{28b}, F. Dittus³², F. Djama⁸⁶, T. Djobava^{53b}, J. I. Djuvsland^{59a}, M. A. B. do Vale^{26c}, D. Dobos³², M. Dobre^{28b}, C. Doglioni⁸², J. Dolejsi¹²⁹, Z. Dolezal¹²⁹, M. Donadelli^{26d}, S. Donati^{124a,124b}, P. Dondero^{121a,121b}, J. Donini³⁶, J. Dopke¹³¹, A. Doria^{104a}, M. T. Dova⁷², A. T. Doyle⁵⁵, E. Drechsler⁵⁶, M. Dris¹⁰, Y. Du^{35d}, J. Duarte-Campderros¹⁵³, E. Duchovni¹⁷¹, G. Duckeck¹⁰⁰, O. A. Ducu^{95,m}, D. Duda¹⁰⁷, A. Dudarev³², A. Chr. Dudder⁸⁴, E. M. Duffield¹⁶, L. Duflo¹¹⁷, M. Dührssen³², M. Dumancic¹⁷¹, M. Dunford^{59a}, H. Duran Yildiz^{4a}, M. Düren⁵⁴, A. Durglishvili^{53b}, D. Duschinger⁴⁶, B. Dutta⁴⁴, M. Dyndal⁴⁴, C. Eckardt⁴⁴, K. M. Ecker¹⁰¹, R. C. Edgar⁹⁰, N. C. Edwards⁴⁸, T. Eifert³², G. Eigen¹⁵, K. Einsweiler¹⁶, T. Ekelof¹⁶⁴, M. El Kacimi^{135c}, V. Ellajosyula⁸⁶, M. Ellert¹⁶⁴, S. Elles⁵, F. Ellinghaus¹⁷⁴, A. A. Elliot¹⁶⁸, N. Ellis³², J. Elmsheuser²⁷, M. Elsing³², D. Emeliyanov¹³¹, Y. Enari¹⁵⁵, O. C. Endner⁸⁴, J. S. Ennis¹⁶⁹, J. Erdmann⁴⁵, A. Ereditato¹⁸, G. Ernis¹⁷⁴, J. Ernst², M. Ernst²⁷, S. Errede¹⁶⁵, E. Ertel⁸⁴, M. Escalier¹¹⁷, H. Esch⁴⁵, C. Escobar¹²⁵, B. Esposito⁴⁹, A. I. Etienne¹³⁶, E. Etzion¹⁵³, H. Evans⁶², A. Ezhilov¹²³, F. Fabbri^{22a,22b}, L. Fabbri^{22a,22b}, G. Facini³³, R. M. Fakhruddinov¹³⁰, S. Falciano^{132a}, R. J. Falla⁷⁹, J. Faltova³², Y. Fang^{35a}, M. Fanti^{92a,92b}, A. Farbin⁸, A. Farilla^{134a}, C. Farina¹²⁵, E. M. Farina^{121a,121b}, T. Farooque¹³, S. Farrell¹⁶, S. M. Farrington¹⁶⁹, P. Farthouat³², F. Fassi^{135e}, P. Fassnacht³², D. Fassouliotis⁹, M. Faucci Giannelli⁷⁸, A. Favareto^{52a,52b}, W. J. Fawcett¹²⁰, L. Fayard¹¹⁷, O. L. Fedin^{123,n}, W. Fedorko¹⁶⁷, S. Feigl¹¹⁹, L. Feligioni⁸⁶, C. Feng^{35d}, E. J. Feng³², H. Feng⁹⁰, A. B. Fenyu¹³⁰, L. Feremenga⁸, P. Fernandez Martinez¹⁶⁶, S. Fernandez Perez¹³, J. Ferrando⁵⁵, A. Ferrari¹⁶⁴, P. Ferrari¹⁰⁷, R. Ferrari^{121a}, D. E. Ferreira de Lima^{59b}, A. Ferrer¹⁶⁶, D. Ferrere⁵¹, C. Ferretti⁹⁰, A. Ferretto Parodi^{52a,52b}, F. Fiedler⁸⁴, A. Filipčić⁷⁶, M. Filipuzzi⁴⁴, F. Filthaut¹⁰⁶, M. Fincke-Keeler¹⁶⁸, K. D. Finelli¹⁵⁰, M. C. N. Fiolhais^{126a,126c}, L. Fiorini¹⁶⁶, A. Firan⁴², A. Fischer², C. Fischer¹³, J. Fischer¹⁷⁴, W. C. Fisher⁹¹, N. Flaschel⁴⁴, I. Fleck¹⁴¹, P. Fleischmann⁹⁰, G. T. Fletcher¹³⁹, R. R. M. Fletcher¹²², T. Flick¹⁷⁴, A. Floderus⁸², L. R. Flores Castillo^{61a}, M. J. Flowerdew¹⁰¹, G. T. Forcolin⁸⁵, A. Formica¹³⁶, A. Forti⁸⁵, A. G. Foster¹⁹, D. Fournier¹¹⁷, H. Fox⁷³, S. Fracchia¹³, P. Francavilla⁸¹, M. Franchini^{22a,22b}, D. Francis³², L. Franconi¹¹⁹, M. Franklin⁵⁸, M. Frate¹⁶², M. Fraternali^{121a,121b}, D. Freeborn⁷⁹, S. M. Fressard-Batraneanu³², F. Friedrich⁴⁶, D. Froidevaux³², J. A. Frost¹²⁰, C. Fukunaga¹⁵⁶, E. Fullana Torregrosa⁸⁴, T. Fusayasu¹⁰², J. Fuster¹⁶⁶, C. Gabaldon⁵⁷, O. Gabizon¹⁷⁴, A. Gabrielli^{22a,22b}, A. Gabrielli¹⁶, G. P. Gach^{40a}, S. Gadatsch³², S. Gadomski⁵¹, G. Gagliardi^{52a,52b}, L. G. Gagnon⁹⁵, P. Gagnon⁶², C. Galea¹⁰⁶, B. Galhardo^{126a,126c}, E. J. Gallas¹²⁰, B. J. Gallop¹³¹, P. Gallus¹²⁸, G. Galster³⁸, K. K. Gan¹¹¹, J. Gao^{35b,86}, Y. Gao⁴⁸, Y. S. Gao^{143,f}, F. M. Garay Walls⁴⁸, C. García¹⁶⁶, J. E. García Navarro¹⁶⁶, M. Garcia-Sciveres¹⁶, R. W. Gardner³³, N. Garelli¹⁴³, V. Garonne¹¹⁹, A. Gascon Bravo⁴⁴, K. Gasnikova⁴⁴, C. Gatti⁴⁹, A. Gaudiello^{52a,52b}, G. Gaudio^{121a}, L. Gauthier⁹⁵, I. L. Gavrilenko⁹⁶, C. Gay¹⁶⁷, G. Gaycken²³, E. N. Gazis¹⁰, Z. Gece¹⁶⁷, C. N. P. Gee¹³¹, Ch. Geich-Gimbel²³, M. Geisen⁸⁴, M. P. Geisler^{59a}, C. Gemme^{52a}, M. H. Genest⁵⁷, C. Geng^{35b,o}, S. Gentile^{132a,132b}, C. Gentsos¹⁵⁴, S. George⁷⁸, D. Gerbaudo¹³, A. Gershon¹⁵³, S. Ghasemi¹⁴¹, H. Ghazlane^{135b}, M. Ghneimat²³, B. Giacobbe^{22a}, S. Giagu^{132a,132b}, P. Giannetti^{124a,124b}, B. Gibbard²⁷, S. M. Gibson⁷⁸, M. Gignac¹⁶⁷, M. Gilchriese¹⁶, T. P. S. Gillam³⁰, D. Gillberg³¹, G. Gilles¹⁷⁴, D. M. Gingrich^{3,d}, N. Giokaris⁹, M. P. Giordani^{163a,163c}, F. M. Giorgi^{22a}, F. M. Giorgi¹⁷, P. F. Giraud¹³⁶, P. Giromini⁵⁸, D. Giugni^{92a}, F. Giuli¹²⁰, C. Giuliani¹⁰¹, M. Giulini^{59b}, B. K. Gjelsten¹¹⁹, S. Gkaitatzis¹⁵⁴, I. Gkialas¹⁵⁴, E. L. Gkoukousis¹¹⁷, L. K. Gladilin⁹⁹, C. Glasman⁸³, J. Glatzer⁵⁰, P. C. F. Glaysheer⁴⁸, A. Glazov⁴⁴, M. Goblirsch-Kolb²⁵, J. Godlewski⁴¹, S. Goldfarb⁸⁹, T. Golling⁵¹, D. Golubkov¹³⁰, A. Gomes^{126a,126b,126d}, R. Gonçalves^{126a}, J. Goncalves Pinto Firmino Da Costa¹³⁶, G. Gonella⁵⁰, L. Gonella¹⁹, A. Gongadze⁶⁶, S. González de la Hoz¹⁶⁶, G. Gonzalez Parra¹³, S. Gonzalez-Sevilla⁵¹, L. Goossens³², P. A. Gorbounov⁹⁷, H. A. Gordon²⁷, I. Gorelov¹⁰⁵, B. Gorini³², E. Gorini^{74a,74b}, A. Gorišek⁷⁶, E. Gornicki⁴¹, A. T. Goshaw⁴⁷, C. Gössling⁴⁵, M. I. Gostkin⁶⁶, C. R. Goudet¹¹⁷, D. Goujdami^{135c}, A. G. Goussiou¹³⁸, N. Govender^{145b,p}, E. Gozani¹⁵², L. Graber⁵⁶, I. Grabowska-Bold^{40a}, P. O. J. Gradin⁵⁷, P. Grafström^{22a,22b}, J. Gramling⁵¹, E. Gramstad¹¹⁹, S. Grancagnolo¹⁷, V. Gratchev¹²³, P. M. Gravila^{28e}, H. M. Gray³², E. Graziani^{134a}, Z. D. Greenwood^{80,q}, C. Grefe²³, K. Gregersen⁷⁹, I. M. Gregor⁴⁴, P. Grenier¹⁴³, K. Grevtsov⁵, J. Griffiths⁸, A. A. Grillo¹³⁷, K. Grimm⁷³, S. Grinstein^{13,r}, Ph. Gris³⁶, J.-F. Grivaz¹¹⁷, S. Groh⁸⁴, J. P. Grohs⁴⁶, E. Gross¹⁷¹, J. Grosse-Knetter⁵⁶, G. C. Grossi⁸⁰, Z. J. Grout⁷⁹, L. Guan⁹⁰, W. Guan¹⁷², J. Guenther⁶³, F. Guescini⁵¹, D. Guest¹⁶², O. Gueta¹⁵³, E. Guido^{52a,52b}, T. Guillemin⁵, S. Guindon², U. Gul⁵⁵, C. Gumpert³², J. Guo^{35e}, Y. Guo^{35b,o}, R. Gupta⁴², S. Gupta¹²⁰, G. Gustavino^{132a,132b}, P. Gutierrez¹¹³, N. G. Gutierrez Ortiz⁷⁹, C. Gutsche⁴⁶, C. Guyot¹³⁶, C. Gwenlan¹²⁰, C. B. Gwilliam⁷⁵, A. Haas¹¹⁰, C. Haber¹⁶, H. K. Hadavand⁸, N. Haddad^{135e}, A. Hadeef⁸⁶, S. Hageböck²³, Z. Hajduk⁴¹, H. Hakobyan^{176,*}, M. Haleem⁴⁴, J. Haley¹¹⁴, G. Halladjian⁹¹, G. D. Hallowell⁸⁶, K. Hamacher¹⁷⁴, P. Hamal¹¹⁵, K. Hamano¹⁶⁸, A. Hamilton^{145a}, G. N. Hamity¹³⁹, P. G. Hamnett⁴⁴, L. Han^{35b}, K. Hanagaki^{67,s}, K. Hanawa¹⁵⁵, M. Hance¹³⁷, B. Haney¹²², S. Hanisch³², P. Hanke^{59a}, R. Hanna¹³⁶, J. B. Hansen³⁸, J. D. Hansen³⁸, M. C. Hansen²³, P. H. Hansen³⁸, K. Hara¹⁶⁰, A. S. Hard¹⁷², T. Harenberg¹⁷⁴, F. Hariri¹¹⁷, S. Harkusha⁹³, R. D. Harrington⁴⁸, P. F. Harrison¹⁶⁹, F. Hartjes¹⁰⁷, N. M. Hartmann¹⁰⁰, M. Hasegawa⁶⁸, Y. Hasegawa¹⁴⁰, A. Hasib¹¹³, S. Hassani¹³⁶, S. Haug¹⁸, R. Hauser⁹¹, L. Hauswald⁴⁶, M. Havranek¹²⁷, C. M. Hawkes¹⁹, R. J. Hawkins³², D. Hayakawa¹⁵⁷,

- D. Hayden⁹¹, C. P. Hays¹²⁰, J. M. Hays⁷⁷, H. S. Hayward⁷⁵, S. J. Haywood¹³¹, S. J. Head¹⁹, T. Heck⁸⁴, V. Hedberg⁸², L. Heelan⁸, S. Heim¹²², T. Heim¹⁶, B. Heinemann¹⁶, J. J. Heinrich¹⁰⁰, L. Heinrich¹¹⁰, C. Heinz⁵⁴, J. Hejbal¹²⁷, L. Helary³², S. Hellman^{146a,146b}, C. Helsens³², J. Henderson¹²⁰, R. C. W. Henderson⁷³, Y. Heng¹⁷², S. Henkelmann¹⁶⁷, A. M. Henriques Correia³², S. Henrot-Versille¹¹⁷, G. H. Herbert¹⁷, V. Hergel¹⁷³, Y. Hernández Jiménez¹⁶⁶, G. Herten⁵⁰, R. Hertenberger¹⁰⁰, L. Hervas³², G. G. Hesketh⁷⁹, N. P. Hessey¹⁰⁷, J. W. Hetherly⁴², R. Hickling⁷⁷, E. Higón-Rodríguez¹⁶⁶, E. Hill¹⁶⁸, J. C. Hill³⁰, K. H. Hiller⁴⁴, S. J. Hillier¹⁹, I. Hinchliffe¹⁶, E. Hines¹²², R. R. Hinman¹⁶, M. Hirose⁵⁰, D. Hirschbuehl¹⁷⁴, J. Hobbs¹⁴⁸, N. Hod^{159a}, M. C. Hodgkinson¹³⁹, P. Hodgson¹³⁹, A. Hoecker³², M. R. Hoferkamp¹⁰⁵, F. Hoenig¹⁰⁰, D. Hohn²³, T. R. Holmes¹⁶, M. Homann⁴⁵, T. M. Hong¹²⁵, B. H. Hooberman¹⁶⁵, W. H. Hopkins¹¹⁶, Y. Horii¹⁰³, A. J. Horton¹⁴², J.-Y. Hostachy⁵⁷, S. Hou¹⁵¹, A. Hoummada^{135a}, J. Howarth⁴⁴, M. Hrabovsky¹¹⁵, I. Hristova¹⁷, J. Hrivnac¹¹⁷, T. Hryn'ova⁵, A. Hrynevich⁹⁴, C. Hsu^{145c}, P. J. Hsu^{151,t}, S.-C. Hsu¹³⁸, D. Hu³⁷, Q. Hu^{35b}, S. Hu^{35e}, Y. Huang⁴⁴, Z. Hubacek¹²⁸, F. Hubaut⁸⁶, F. Huegging²³, T. B. Huffman¹²⁰, E. W. Hughes³⁷, G. Hughes⁷³, M. Huhtinen³², P. Huo¹⁴⁸, N. Huseynov^{66,b}, J. Huston⁹¹, J. Huth⁵⁸, G. Iacobucci⁵¹, G. Iakovidis²⁷, I. Ibragimov¹⁴¹, L. Iconomidou-Fayard¹¹⁷, E. Ideal¹⁷⁵, Z. Idrissi^{135e}, P. Iengo³², O. Igonkina^{107,u}, T. Iizawa¹⁷⁰, Y. Ikegami⁶⁷, M. Ikeno⁶⁷, Y. Ilchenko^{11,v}, D. Iliadis¹⁵⁴, N. Ilic¹⁴³, T. Ince¹⁰¹, G. Introzzi^{121a,121b}, P. Ioannou^{9,*}, M. Iodice^{134a}, K. Iordanidou³⁷, V. Ippolito⁵⁸, N. Ishijima¹¹⁸, M. Ishino¹⁵⁵, M. Ishitsuka¹⁵⁷, R. Ishmukhametov¹¹¹, C. Issever¹²⁰, S. Istin^{20a}, F. Ito¹⁶⁰, J. M. Iturbe Ponce⁸⁵, R. Iuppa^{133a,133b}, W. Iwanski⁴¹, H. Iwasaki⁶⁷, J. M. Izen⁴³, V. Izzo^{104a}, S. Jabbar³, B. Jackson¹²², P. Jackson¹, V. Jain², K. B. Jakobi⁸⁴, K. Jakobs⁵⁰, S. Jakobsen³², T. Jakoubek¹²⁷, D. O. Jamin¹¹⁴, D. K. Jana⁸⁰, E. Jansen⁷⁹, R. Jansky⁶³, J. Janssen²³, M. Janus⁵⁶, G. Jarlskog⁸², N. Javadov^{66,b}, T. Javůrek⁵⁰, F. Jeanneau¹³⁶, L. Jeanty¹⁶, J. Jejelava^{53a,w}, G.-Y. Jeng¹⁵⁰, D. Jennens⁸⁹, P. Jenni^{50,x}, C. Jeske¹⁶⁹, S. Jézéquel⁵, H. Ji¹⁷², J. Jia¹⁴⁸, H. Jiang⁶⁵, Y. Jiang^{35b}, S. Jiggins⁷⁹, J. Jimenez Pena¹⁶⁶, S. Jin^{35a}, A. Jinaru^{28b}, O. Jinnouchi¹⁵⁷, P. Johansson¹³⁹, K. A. Johns⁷, W. J. Johnson¹³⁸, K. Jon-And^{146a,146b}, G. Jones¹⁶⁹, R. W. L. Jones⁷³, S. Jones⁷, T. J. Jones⁷⁵, J. Jongmanns^{59a}, P. M. Jorge^{126a,126b}, J. Jovicevic^{159a}, X. Ju¹⁷², A. Juste Rozas^{13,r}, M. K. Köhler¹⁷¹, A. Kaczmarek⁴¹, M. Kado¹¹⁷, H. Kagan¹¹¹, M. Kagan¹⁴³, S. J. Kahn⁸⁶, T. Kaji¹⁷⁰, E. Kajomovitz⁴⁷, C. W. Kalderon¹²⁰, A. Kaluza⁸⁴, S. Kama⁴², A. Kamenshchikov¹³⁰, N. Kanaya¹⁵⁵, S. Kaneti³⁰, L. Kanjir⁷⁶, V. A. Kantserov⁹⁸, J. Kanzaki⁶⁷, B. Kaplan¹¹⁰, L. S. Kaplan¹⁷², A. Kapliy³³, D. Kar^{145c}, K. Karakostas¹⁰, A. Karamaoun³, N. Karastathis¹⁰, M. J. Kareem⁵⁶, E. Karentzos¹⁰, M. Karnevskiy⁸⁴, S. N. Karpov⁶⁶, Z. M. Karpova⁶⁶, K. Karthik¹¹⁰, V. Kartvelishvili⁷³, A. N. Karyukhin¹³⁰, K. Kasahara¹⁶⁰, L. Kashif¹⁷², R. D. Kass¹¹¹, A. Kastanas¹⁵, Y. Kataoka¹⁵⁵, C. Kato¹⁵⁵, A. Katre⁵¹, J. Katzy⁴⁴, K. Kawagoe⁷¹, T. Kawamoto¹⁵⁵, G. Kawamura⁵⁶, V. F. Kazanin^{109,c}, R. Keeler¹⁶⁸, R. Kehoe⁴², J. S. Keller⁴⁴, J. J. Kempster⁷⁸, K. Kentaro¹⁰³, H. Keoshkerian¹⁵⁸, O. Kepka¹²⁷, B. P. Kerševan⁷⁶, S. Kersten¹⁷⁴, R. A. Keyes⁸⁸, M. Khader¹⁶⁵, F. Khalil-zada¹², A. Khanov¹¹⁴, A. G. Kharlamov^{109,c}, T. J. Khoo⁵¹, V. Khovanskiy⁹⁷, E. Khramov⁶⁶, J. Khubua^{53b,y}, S. Kido⁶⁸, C. R. Kilby⁷⁸, H. Y. Kim⁸, S. H. Kim¹⁶⁰, Y. K. Kim³³, N. Kimura¹⁵⁴, O. M. Kind¹⁷, B. T. King⁷⁵, M. King¹⁶⁶, S. B. King¹⁶⁷, J. Kirk¹³¹, A. E. Kiryunin¹⁰¹, T. Kishimoto¹⁵⁵, D. Kisielewska^{40a}, F. Kiss⁵⁰, K. Kiuchi¹⁶⁰, O. Kivernyk¹³⁶, E. Kladiva^{144b}, M. H. Klein³⁷, M. Klein⁷⁵, U. Klein⁷⁵, K. Kleinknecht⁸⁴, P. Klimek¹⁰⁸, A. Klimentov²⁷, R. Klingenberg⁴⁵, J. A. Klinger¹³⁹, T. Klioutchnikova³², E.-E. Kluge^{59a}, P. Kluit¹⁰⁷, S. Kluth¹⁰¹, J. Knapik⁴¹, E. Kneringer⁶³, E. B. F. G. Knoop⁸⁶, A. Knue⁵⁵, A. Kobayashi¹⁵⁵, D. Kobayashi¹⁵⁷, T. Kobayashi¹⁵⁵, M. Kobel⁴⁶, M. Kocian¹⁴³, P. Kodys¹²⁹, N. M. Koehler¹⁰¹, T. Koffas³¹, E. Koffeman¹⁰⁷, T. Koi¹⁴³, H. Kolanoski¹⁷, M. Kolb^{59b}, I. Koletsou⁵, A. A. Komar^{96,*}, Y. Komori¹⁵⁵, T. Kondo⁶⁷, N. Kondrashova⁴⁴, K. Köneke⁵⁰, A. C. König¹⁰⁶, T. Kono^{67,z}, R. Konoplich^{110,aa}, N. Konstantinidis⁷⁹, R. Kopeliansky⁶², S. Koperny^{40a}, L. Köpke⁸⁴, A. K. Kopp⁵⁰, K. Korcyl⁴¹, K. Kordas¹⁵⁴, A. Korn⁷⁹, A. A. Korol^{109,c}, I. Korolkov¹³, E. V. Korolkova¹³⁹, O. Kortner¹⁰¹, S. Kortner¹⁰¹, T. Kosek¹²⁹, V. V. Kostyukhin²³, A. Kotwal⁴⁷, A. Kourkoumeli-Charalampidi^{121a,121b}, C. Kourkoumelis⁹, V. Kouskoura²⁷, A. B. Kowalewska⁴¹, R. Kowalewski¹⁶⁸, T. Z. Kowalski^{40a}, C. Kozakai¹⁵⁵, W. Kozanecki¹³⁶, A. S. Kozhin¹³⁰, V. A. Kramarenko⁹⁹, G. Kramberger⁷⁶, D. Krasnopevtsev⁹⁸, M. W. Krasny⁸¹, A. Krasznahorkay³², A. Kravchenko²⁷, M. Kretz^{59c}, J. Kretzschmar⁷⁵, K. Kreutzfeldt⁵⁴, P. Krieger¹⁵⁸, K. Krizka³³, K. Kroeninger⁴⁵, H. Kroha¹⁰¹, J. Kroll¹²², J. Kroseberg²³, J. Krstic¹⁴, U. Kruchonak⁶⁶, H. Krüger²³, N. Krumnack⁶⁵, A. Kruse¹⁷², M. C. Kruse⁴⁷, M. Kruskal²⁴, T. Kubota⁸⁹, H. Kucuk⁷⁹, S. Kudah^{4b}, J. T. Kuechler¹⁷⁴, S. Kuehn⁵⁰, A. Kugel^{59c}, F. Kuger¹⁷³, A. Kuhl¹³⁷, T. Kuhl⁴⁴, V. Kukhtin⁶⁶, R. Kukla¹³⁶, Y. Kulchitsky⁹³, S. Kuleshov^{34b}, M. Kuna^{132a,132b}, T. Kunigo⁶⁹, A. Kupco¹²⁷, H. Kurashige⁶⁸, Y. A. Kurochkin⁹³, V. Kus¹²⁷, E. S. Kuwertz¹⁶⁸, M. Kuze¹⁵⁷, J. Kvita¹¹⁵, T. Kwan¹⁶⁸, D. Kyriazopoulos¹³⁹, A. La Rosa¹⁰¹, J. L. La Rosa Navarro^{26d}, L. La Rotonda^{39a,39b}, C. Lacasta¹⁶⁶, F. Lacava^{132a,132b}, J. Lacey³¹, H. Lacker¹⁷, D. Lacour⁸¹, V. R. Lacuesta¹⁶⁶, E. Ladygin⁶⁶, R. Lafaye⁵, B. Laforge⁸¹, T. Lagouri¹⁷⁵, S. Lai⁵⁶, S. Lammers⁶², W. Lampl⁷, E. Lançon¹³⁶, U. Landgraf⁵⁰, M. P. J. Landon⁷⁷, M. C. Lanfermann⁵¹, V. S. Lang^{59a}, J. C. Lange¹³, A. J. Lankford¹⁶², F. Lanni²⁷, K. Lantzsche²³, A. Lanza^{121a}, S. Laplace⁸¹, C. Lapoire³², J. F. Laporte¹³⁶, T. Lari^{92a}, F. Lasagni Manghi^{22a,22b}, M. Lassnig³², P. Laurelli⁴⁹, W. Lavrijsen¹⁶, A. T. Law¹³⁷, P. Laycock⁷⁵, T. Lazovich⁵⁸, M. Lazzaroni^{92a,92b}, B. Le⁸⁹, O. Le Dortz⁸¹, E. Le Guirriec⁸⁶, E. P. Le Quilleuc¹³⁶, M. LeBlanc¹⁶⁸, T. LeCompte⁶, F. Ledroit-Guillon⁵⁷, C. A. Lee²⁷, S. C. Lee¹⁵¹, L. Lee¹, B. Lefebvre⁸⁸, G. Lefebvre⁸¹,

- M. Lefebvre¹⁶⁸, F. Legger¹⁰⁰, C. Leggett¹⁶, A. Lehan⁷⁵, G. Lehmann Miotto³², X. Lei⁷, W. A. Leight³¹, A. Leisos^{154,ab}, A. G. Leister¹⁷⁵, M. A. L. Leite^{26d}, R. Leitner¹²⁹, D. Lellouch¹⁷¹, B. Lemmer⁵⁶, K. J. C. Leney⁷⁹, T. Lenz²³, B. Lenzi³², R. Leone⁷, S. Leone^{124a,124b}, C. Leonidopoulos⁴⁸, S. Leontsinis¹⁰, G. Lerner¹⁴⁹, C. Leroy⁹⁵, A. A. J. Lesage¹³⁶, C. G. Lester³⁰, M. Levchenko¹²³, J. Levêque⁵, D. Levin⁹⁰, L. J. Levinson¹⁷¹, M. Levy¹⁹, D. Lewis⁷⁷, A. M. Leyko²³, M. Leyton⁴³, B. Li^{35b,o}, C. Li^{35b}, H. Li¹⁴⁸, H. L. Li³³, L. Li⁴⁷, L. Li^{35e}, Q. Li^{35a}, S. Li⁴⁷, X. Li⁸⁵, Y. Li¹⁴¹, Z. Liang^{35a}, B. Liberti^{133a}, A. Liblong¹⁵⁸, P. Lichard³², K. Lie¹⁶⁵, J. Liebal²³, W. Liebig¹⁵, A. Limosani¹⁵⁰, S. C. Lin^{151,ac}, T. H. Lin⁸⁴, B. E. Lindquist¹⁴⁸, A. E. Lioni⁵¹, E. Lipeles¹²², A. Lipniacka¹⁵, M. Lisovyi^{59b}, T. M. Liss¹⁶⁵, A. Lister¹⁶⁷, A. M. Litke¹³⁷, B. Liu^{151,ad}, D. Liu¹⁵¹, H. Liu⁹⁰, H. Liu²⁷, J. Liu⁸⁶, J. B. Liu^{35b}, K. Liu⁸⁶, L. Liu¹⁶⁵, M. Liu⁴⁷, M. Liu^{35b}, Y. L. Liu^{35b}, Y. Liu^{35b}, M. Livan^{121a,121b}, A. Lleres⁵⁷, J. Llorente Merino^{35a}, S. L. Lloyd⁷⁷, F. Lo Sterzo¹⁵¹, E. Lobodzinska⁴⁴, P. Loch⁷, W. S. Lockman¹³⁷, F. K. Loebinger⁸⁵, A. E. Loevschall-Jensen³⁸, K. M. Loew²⁵, A. Loginov^{175,*}, T. Lohse¹⁷, K. Lohwasser⁴⁴, M. Lokajicek¹²⁷, B. A. Long²⁴, J. D. Long¹⁶⁵, R. E. Long⁷³, L. Longo^{74a,74b}, K. A. Looper¹¹¹, L. Lopes^{126a}, D. Lopez Mateos⁵⁸, B. Lopez Paredes¹³⁹, I. Lopez Paz¹³, A. Lopez Solis⁸¹, J. Lorenz¹⁰⁰, N. Lorenzo Martinez⁶², M. Losada²¹, P. J. Lösel¹⁰⁰, X. Lou^{35a}, A. Lounis¹¹⁷, J. Love⁶, P. A. Love⁷³, H. Lu^{61a}, N. Lu⁹⁰, H. J. Lubatti¹³⁸, C. Luci^{132a,132b}, A. Lucotte⁵⁷, C. Luedtke⁵⁰, F. Luehring⁶², W. Lukas⁶³, L. Luminari^{132a}, O. Lundberg^{146a,146b}, B. Lund-Jensen¹⁴⁷, P. M. Luzzi⁸¹, D. Lynn²⁷, R. Lysak¹²⁷, E. Lytken⁸², V. Lyubushkin⁶⁶, H. Ma²⁷, L. L. Ma^{35d}, Y. Ma^{35d}, G. Maccarrone⁴⁹, A. Macchiolo¹⁰¹, C. M. Macdonald¹³⁹, B. Maček⁷⁶, J. Machado Miguens^{122,126b}, D. Madaffari⁸⁶, R. Madar³⁶, H. J. Maddocks¹⁶⁴, W. F. Mader⁴⁶, A. Madsen⁴⁴, J. Maeda⁶⁸, S. Maeland¹⁵, T. Maeno²⁷, A. Maevskiy⁹⁹, E. Magradze⁵⁶, J. Mahlstedt¹⁰⁷, C. Maiani¹¹⁷, C. Maidantchik^{26a}, A. A. Maier¹⁰¹, T. Maier¹⁰⁰, A. Maio^{126a,126b,126d}, S. Majewski¹¹⁶, Y. Makida⁶⁷, N. Makovec¹¹⁷, B. Malaescu⁸¹, Pa. Malecki⁴¹, V. P. Maleev¹²³, F. Malek⁵⁷, U. Mallik⁶⁴, D. Malon⁶, C. Malone¹⁴³, S. Maltezos¹⁰, S. Malyukov³², J. Mamuzic¹⁶⁶, G. Mancini⁴⁹, B. Mandelli³², L. Mandelli^{92a}, I. Mandić⁷⁶, J. Maneira^{126a,126b}, L. Manhaes de Andrade Filho^{26b}, J. Manjarres Ramos^{159b}, A. Mann¹⁰⁰, A. Manousos³², B. Mansoulie¹³⁶, J. D. Mansour^{35a}, R. Mantifel⁸⁸, M. Mantoani⁵⁶, S. Manzoni^{92a,92b}, L. Mapelli³², G. Marceca²⁹, L. March⁵¹, G. Marchiori⁸¹, M. Marcisovsky¹²⁷, M. Marjanovic¹⁴, D. E. Marley⁹⁰, F. Marroquim^{26a}, S. P. Marsden⁸⁵, Z. Marshall¹⁶, S. Marti-Garcia¹⁶⁶, B. Martin⁹¹, T. A. Martin¹⁶⁹, V. J. Martin⁴⁸, B. Martin dit Latour¹⁵, M. Martinez^{13,r}, V. I. Martinez Outschoorn¹⁶⁵, S. Martin-Haugh¹³¹, V. S. Martoiu^{28b}, A. C. Martyniuk⁷⁹, M. Marx¹³⁸, A. Marzin³², L. Masetti⁸⁴, T. Mashimo¹⁵⁵, R. Mashinistov⁹⁶, J. Masik⁸⁵, A. L. Maslennikov^{109,c}, I. Massa^{22a,22b}, L. Massa^{22a,22b}, P. Mastrandrea⁵, A. Mastroberardino^{39a,39b}, T. Masubuchi¹⁵⁵, P. Mättig¹⁷⁴, J. Mattmann⁸⁴, J. Maurer^{28b}, S. J. Maxfield⁷⁵, D. A. Maximov^{109,c}, R. Mazini¹⁵¹, S. M. Mazza^{92a,92b}, N. C. Mc Fadden¹⁰⁵, G. Mc Goldrick¹⁵⁸, S. P. Mc Kee⁹⁰, A. McCann⁹⁰, R. L. McCarthy¹⁴⁸, T. G. McCarthy¹⁰¹, L. I. McClymont⁷⁹, E. F. McDonald⁸⁹, J. A. Mcfayden⁷⁹, G. Mchedlidze⁵⁶, S. J. McMahon¹³¹, R. A. McPherson^{168,1}, M. Medinnis⁴⁴, S. Meehan¹³⁸, S. Mehlhase¹⁰⁰, A. Mehta⁷⁵, K. Meier^{59a}, C. Meineck¹⁰⁰, B. Meirose⁴³, D. Melini¹⁶⁶, B. R. Mellado Garcia^{145c}, M. Melo^{144a}, F. Meloni¹⁸, A. Mengarelli^{22a,22b}, S. Menke¹⁰¹, E. Meoni¹⁶¹, S. Mergelmeyer¹⁷, P. Mermod⁵¹, L. Merola^{104a,104b}, C. Meroni^{92a}, F. S. Merritt³³, A. Messina^{132a,132b}, J. Metcalfe⁶, A. S. Mete¹⁶², C. Meyer⁸⁴, C. Meyer¹²², J.-P. Meyer¹³⁶, J. Meyer¹⁰⁷, H. Meyer Zu Theenhausen^{59a}, F. Miano¹⁴⁹, R. P. Middleton¹³¹, S. Miglioranza^{52a,52b}, L. Mijović⁴⁸, G. Mikenberg¹⁷¹, M. Mikestikova¹²⁷, M. Mikuz⁷⁶, M. Milesi⁸⁹, A. Milic⁶³, D. W. Miller³³, C. Mills⁴⁸, A. Milov¹⁷¹, D. A. Milstead^{146a,146b}, A. A. Minaenko¹³⁰, Y. Minami¹⁵⁵, I. A. Minashvili⁶⁶, A. I. Mincer¹¹⁰, B. Mindur^{40a}, M. Mineev⁶⁶, Y. Ming¹⁷², L. M. Mir¹³, K. P. Mistry¹²², T. Mitani¹⁷⁰, J. Mitrevski¹⁰⁰, V. A. Mitsou¹⁶⁶, A. Miucci¹⁸, P. S. Miyagawa¹³⁹, J. U. Mjörnmark⁸², T. Moa^{146a,146b}, K. Mochizuki⁹⁵, S. Mohapatra³⁷, S. Molander^{146a,146b}, R. Moles-Valls²³, R. Monden⁶⁹, M. C. Mondragon⁹¹, K. Mönig⁴⁴, J. Monk³⁸, E. Monnier⁸⁶, A. Montalbano¹⁴⁸, J. Montejo Berlingen³², F. Monticelli⁷², S. Monzani^{92a,92b}, R. W. Moore³, N. Morange¹¹⁷, D. Moreno²¹, M. Moreno Llacer⁵⁶, P. Morettini^{52a}, D. Mori¹⁴², T. Mori¹⁵⁵, M. Morii⁵⁸, M. Morinaga¹⁵⁵, V. Morisbak¹¹⁹, S. Moritz⁸⁴, A. K. Morley¹⁵⁰, G. Mornacchi³², J. D. Morris⁷⁷, S. S. Mortensen³⁸, L. Morvaj¹⁴⁸, M. Mosidze^{53b}, J. Moss¹⁴³, K. Motohashi¹⁵⁷, R. Mount¹⁴³, E. Mountricha²⁷, S. V. Mouraviev^{96,*}, E. J. W. Moyse⁸⁷, S. Muanza⁸⁶, R. D. Mudd¹⁹, F. Mueller¹⁰¹, J. Mueller¹²⁵, R. S. P. Mueller¹⁰⁰, T. Mueller³⁰, D. Muenstermann⁷³, P. Mullen⁵⁵, G. A. Mullier¹⁸, F. J. Munoz Sanchez⁸⁵, J. A. Murillo Quijada¹⁹, W. J. Murray^{169,131}, H. Musheghyan⁵⁶, M. Muškinja⁷⁶, A. G. Myagkov^{130,ae}, M. Myska¹²⁸, B. P. Nachman¹⁴³, O. Nackenhorst⁵¹, K. Nagai¹²⁰, R. Nagai^{67,z}, K. Nagano⁶⁷, Y. Nagasaka⁶⁰, K. Nagata¹⁶⁰, M. Nagel⁵⁰, E. Nagy⁸⁶, A. M. Nairz³², Y. Nakahama¹⁰³, K. Nakamura⁶⁷, T. Nakamura¹⁵⁵, I. Nakano¹¹², H. Namasivayam⁴³, R. F. Naranjo Garcia⁴⁴, R. Narayan¹¹, D. I. Narrias Villar^{59a}, I. Naryshkin¹²³, T. Naumann⁴⁴, G. Navarro²¹, R. Nayyar⁷, H. A. Neal⁹⁰, P. Yu. Nechaeva⁹⁶, T. J. Neep⁸⁵, A. Negri^{121a,121b}, M. Negrini^{22a}, S. Nektarijevic¹⁰⁶, C. Nellist¹¹⁷, A. Nelson¹⁶², S. Nemecek¹²⁷, P. Nemethy¹¹⁰, A. A. Nepomuceno^{26a}, M. Nessi^{32,af}, M. S. Neubauer¹⁶⁵, M. Neumann¹⁷⁴, R. M. Neves¹¹⁰, P. Nevski²⁷, P. R. Newman¹⁹, D. H. Nguyen⁶, T. Nguyen Manh⁹⁵, R. B. Nickerson¹²⁰, R. Nicolaidou¹³⁶, J. Nielsen¹³⁷, A. Nikiforov¹⁷, V. Nikolaenko^{130,ae}, I. Nikolic-Audit⁸¹, K. Nikolopoulos¹⁹, J. K. Nilsen¹¹⁹, P. Nilsson²⁷, Y. Ninomiya¹⁵⁵, A. Nisati^{132a}, R. Nisius¹⁰¹, T. Nobe¹⁵⁵, M. Nomachi¹¹⁸,

- I. Nomidis³¹, T. Nooney⁷⁷, S. Norberg¹¹³, M. Nordberg³², N. Norjoharuddeen¹²⁰, O. Novgorodova⁴⁶, S. Nowak¹⁰¹, M. Nozaki⁶⁷, L. Nozka¹¹⁵, K. Ntekas¹⁰, E. Nurse⁷⁹, F. Nuti⁸⁹, F. O'grady⁷, D. C. O'Neil¹⁴², A. A. O'Rourke⁴⁴, V. O'Shea⁵⁵, F. G. Oakham^{31,d}, H. Oberlack¹⁰¹, T. Obermann²³, J. Ocariz⁸¹, A. Ochi⁶⁸, I. Ochoa³⁷, J. P. Ochoa-Ricoux^{34a}, S. Oda⁷¹, S. Odaka⁶⁷, H. Ogren⁶², A. Oh⁸⁵, S. H. Oh⁴⁷, C. C. Ohm¹⁶, H. Ohman¹⁶⁴, H. Oide³², H. Okawa¹⁶⁰, Y. Okumura¹⁵⁵, T. Okuyama⁶⁷, A. Olariu^{28b}, L. F. Oleiro Seabra^{126a}, S. A. Olivares Pino⁴⁸, D. Oliveira Damazio²⁷, A. Olszewski⁴¹, J. Olszowska⁴¹, A. Onofre^{126a,126e}, K. Onogi¹⁰³, P. U. E. Onyisi^{11,v}, M. J. Oreglia³³, Y. Oren¹⁵³, D. Orestano^{134a,134b}, N. Orlando^{61b}, R. S. Orr¹⁵⁸, B. Osculati^{52a,52b}, R. Ospanov⁸⁵, G. Otero y Garzon²⁹, H. Otono⁷¹, M. Ouchrif^{135d}, F. Ould-Saada¹¹⁹, A. Ouraou¹³⁶, K. P. Oussoren¹⁰⁷, Q. Ouyang^{35a}, M. Owen⁵⁵, R. E. Owen¹⁹, V. E. Ozcan^{20a}, N. Ozturk⁸, K. Pachal¹⁴², A. Pacheco Pages¹³, L. Pacheco Rodriguez¹³⁶, C. Padilla Aranda¹³, M. Pagáčová⁵⁰, S. Pagan Griso¹⁶, F. Paige²⁷, P. Pais⁸⁷, K. Pajchel¹¹⁹, G. Palacino^{159b}, S. Palazzo^{39a,39b}, S. Palestini³², M. Palka^{40b}, D. Pallin³⁶, E. St. Panagiotopoulou¹⁰, C. E. Pandini⁸¹, J. G. Panduro Vazquez⁷⁸, P. Pani^{146a,146b}, S. Panitkin²⁷, D. Pantea^{28b}, L. Paolozzi⁵¹, Th. D. Papadopoulou¹⁰, K. Papageorgiou¹⁵⁴, A. Paramonov⁶, D. Paredes Hernandez¹⁷⁵, A. J. Parker⁷³, M. A. Parker³⁰, K. A. Parker¹³⁹, F. Parodi^{52a,52b}, J. A. Parsons³⁷, U. Parzefall⁵⁰, V. R. Pascuzzi¹⁵⁸, E. Pasqualucci^{132a}, S. Passaggio^{52a}, Fr. Pastore⁷⁸, G. Pásztor^{31,ag}, S. Patariaia¹⁷⁴, J. R. Pater⁸⁵, T. Pauly³², J. Pearce¹⁶⁸, B. Pearson¹¹³, L. E. Pedersen³⁸, M. Pedersen¹¹⁹, S. Pedraza Lopez¹⁶⁶, R. Pedro^{126a,126b}, S. V. Peleganchuk^{109,c}, O. Penc¹²⁷, C. Peng^{35a}, H. Peng^{35b}, J. Penwell⁶², B. S. Peralva^{26b}, M. M. Perego¹³⁶, D. V. Perepelitsa²⁷, E. Perez Codina^{159a}, L. Perini^{92a,92b}, H. Pernegger³², S. Perrella^{104a,104b}, R. Peschke⁴⁴, V. D. Peshekhonov⁶⁶, K. Peters⁴⁴, R. F. Y. Peters⁸⁵, B. A. Petersen³², T. C. Petersen³⁸, E. Petit⁵⁷, A. Petridis¹, C. Petridou¹⁵⁴, P. Petroff¹¹⁷, E. Petrolo^{132a}, M. Petrov¹²⁰, F. Petrucci^{134a,134b}, N. E. Pettersson⁸⁷, A. Peyaud¹³⁶, R. Pezoa^{34b}, P. W. Phillips¹³¹, G. Piacquadio^{143,ah}, E. Pianori¹⁶⁹, A. Picazio⁸⁷, E. Piccaro⁷⁷, M. Piccinini^{22a,22b}, M. A. Pickering¹²⁰, R. Piegai²⁹, J. E. Pilcher³³, A. D. Pilkington⁸⁵, A. W. J. Pin⁸⁵, M. Pinamonti^{163a,163c,ai}, J. L. Pinfold³, A. Pingel³⁸, S. Pires⁸¹, H. Pirumov⁴⁴, M. Pitt¹⁷¹, L. Plazak^{144a}, M.-A. Pleier²⁷, V. Pleskot⁸⁴, E. Plotnikova⁶⁶, P. Plucinski⁹¹, D. Pluth⁶⁵, R. Poettgen^{146a,146b}, L. Poggioli¹¹⁷, D. Pohl²³, G. Polesello^{121a}, A. Poley⁴⁴, A. Policicchio^{39a,39b}, R. Polifka¹⁵⁸, A. Polini^{22a}, C. S. Pollard⁵⁵, V. Polychronakos²⁷, K. Pommès³², L. Pontecorvo^{132a}, B. G. Pope⁹¹, G. A. Popeneciu^{28c}, D. S. Popovic¹⁴, A. Poppleton³², S. Pospisil¹²⁸, K. Potamianos¹⁶, I. N. Potrap⁶⁶, C. J. Potter³⁰, C. T. Potter¹¹⁶, G. Poulard³², J. Poveda³², V. Pozdnyakov⁶⁶, M. E. Pozo Astigarraga³², P. Pralavorio⁸⁶, A. Pranko¹⁶, S. Prell⁶⁵, D. Price⁸⁵, L. E. Price⁶, M. Primavera^{74a}, S. Prince⁸⁸, K. Prokofiev^{61c}, F. Prokoshin^{34b}, S. Protopopescu²⁷, J. Proudfoot⁶, M. Przybycien^{40a}, D. Puddu^{134a,134b}, M. Purohit^{27,aj}, P. Puzo¹¹⁷, J. Qian⁹⁰, G. Qin⁵⁵, Y. Qin⁸⁵, A. Quadt⁵⁶, W. B. Quayle^{163a,163b}, M. Queitsch-Maitland⁸⁵, D. Quilty⁵⁵, S. Raddum¹¹⁹, V. Radeka²⁷, V. Radescu¹²⁰, S. K. Radhakrishnan¹⁴⁸, P. Radloff¹¹⁶, P. Rados⁸⁹, F. Ragusa^{92a,92b}, G. Rahal¹⁷⁷, J. A. Raine⁸⁵, S. Rajagopalan²⁷, M. Rammensee³², C. Rangel-Smith¹⁶⁴, M. G. Ratti^{92a,92b}, F. Rauscher¹⁰⁰, S. Rave⁸⁴, T. Ravenscroft⁵⁵, I. Ravinovich¹⁷¹, M. Raymond³², A. L. Read¹¹⁹, N. P. Readioff⁷⁵, M. Reale^{74a,74b}, D. M. Rebuffi^{121a,121b}, A. Redelbach¹⁷³, G. Redlinger²⁷, R. Reece¹³⁷, K. Reeves⁴³, L. Rehnisch¹⁷, J. Reichert¹²², H. Reisin²⁹, C. Rembser³², H. Ren^{35a}, M. Rescigno^{132a}, S. Resconi^{92a}, O. L. Rezanova^{109,c}, P. Reznicek¹²⁹, R. Rezvani⁹⁵, R. Richter¹⁰¹, S. Richter⁷⁹, E. Richter-Was^{40b}, O. Ricken²³, M. Ridel⁸¹, P. Rieck¹⁷, C. J. Riegel¹⁷⁴, J. Rieger⁵⁶, O. Rifki¹¹³, M. Rijssenbeek¹⁴⁸, A. Rimoldi^{121a,121b}, M. Rimoldi¹⁸, L. Rinaldi^{22a}, B. Ristic⁵¹, E. Ritsch³², I. Riu¹³, F. Rizatdinova¹¹⁴, E. Rizvi⁷⁷, C. Rizzi¹³, S. H. Robertson^{88,1}, A. Robichaud-Veronneau⁸⁸, D. Robinson³⁰, J. E. M. Robinson⁴⁴, A. Robson⁵⁵, C. Roda^{124a,124b}, Y. Rodina⁸⁶, A. Rodriguez Perez¹³, D. Rodriguez Rodriguez¹⁶⁶, S. Roe³², C. S. Rogan⁵⁸, O. Røhne¹¹⁹, A. Romaniouk⁹⁸, M. Romano^{22a,22b}, S. M. Romano Saez³⁶, E. Romero Adam¹⁶⁶, N. Rompotis¹³⁸, M. Ronzani⁵⁰, L. Roos⁸¹, E. Ros¹⁶⁶, S. Rosati^{132a}, K. Rosbach⁵⁰, P. Rose¹³⁷, O. Rosenthal¹⁴¹, N.-A. Rosien⁵⁶, V. Rossetti^{146a,146b}, E. Rossi^{104a,104b}, L. P. Rossi^{52a}, J. H. N. Rosten³⁰, R. Rosten¹³⁸, M. Rotaru^{28b}, I. Roth¹⁷¹, J. Rothberg¹³⁸, D. Rousseau¹¹⁷, C. R. Royon¹³⁶, A. Rozanov⁸⁶, Y. Rozen¹⁵², X. Ruan^{145c}, F. Rubbo¹⁴³, M. S. Rudolph¹⁵⁸, F. Rühr⁵⁰, A. Ruiz-Martinez³¹, Z. Rurikova⁵⁰, N. A. Rusakovich⁶⁶, A. Ruschke¹⁰⁰, H. L. Russell¹³⁸, J. P. Rutherford⁷, N. Ruthmann³², Y. F. Ryabov¹²³, M. Rybar¹⁶⁵, G. Rybkin¹¹⁷, S. Ryu⁶, A. Ryzhov¹³⁰, G. F. Rzehorz⁵⁶, A. F. Saavedra¹⁵⁰, G. Sabato¹⁰⁷, S. Sacerdoti²⁹, H. F.-W. Sadrozinski¹³⁷, R. Sadykov⁶⁶, F. Safai Tehrani^{132a}, P. Saha¹⁰⁸, M. Sahinsoy^{59a}, M. Saimpert¹³⁶, T. Saito¹⁵⁵, H. Sakamoto¹⁵⁵, Y. Sakurai¹⁷⁰, G. Salamanna^{134a,134b}, A. Salamon^{133a,133b}, J. E. Salazar Loyola^{34b}, D. Salek¹⁰⁷, P. H. Sales De Bruin¹³⁸, D. Salihagic¹⁰¹, A. Salnikov¹⁴³, J. Salt¹⁶⁶, D. Salvatore^{39a,39b}, F. Salvatore¹⁴⁹, A. Salvucci^{61a}, A. Salzburger³², D. Sammel⁵⁰, D. Sampsonidis¹⁵⁴, A. Sanchez^{104a,104b}, J. Sánchez¹⁶⁶, V. Sanchez Martinez¹⁶⁶, H. Sandaker¹¹⁹, R. L. Sandbach⁷⁷, H. G. Sander⁸⁴, M. Sandhoff¹⁷⁴, C. Sandoval²¹, R. Sandstroem¹⁰¹, D. P. C. Sankey¹³¹, M. Sannino^{52a,52b}, A. Sansoni⁴⁹, C. Santoni³⁶, R. Santonico^{133a,133b}, H. Santos^{126a}, I. Santoyo Castillo¹⁴⁹, K. Sapp¹²⁵, A. Sapronov⁶⁶, J. G. Saraiva^{126a,126d}, B. Sarrazin²³, O. Sasaki⁶⁷, Y. Sasaki¹⁵⁵, K. Sato¹⁶⁰, G. Sauvage^{5,*}, E. Sauvan⁵, G. Savage⁷⁸, P. Savard^{158,d}, N. Savic¹⁰¹, C. Sawyer¹³¹, L. Sawyer^{80,q}, J. Saxon³³, C. Sbarra^{22a}, A. Sbrizzi^{22a,22b}, T. Scanlon⁷⁹, D. A. Scannicchio¹⁶², M. Scarcella¹⁵⁰, V. Scarfone^{39a,39b}, J. Schaarschmidt¹⁷¹, P. Schacht¹⁰¹, B. M. Schachtner¹⁰⁰, D. Schaefer³², L. Schaefer¹²², R. Schaefer⁴⁴

J. Schaeffer⁸⁴, S. Schaepe²³, S. Schaetzel^{59b}, U. Schäfer⁸⁴, A. C. Schaffer¹¹⁷, D. Schaile¹⁰⁰, R. D. Schamberger¹⁴⁸, V. Scharf^{59a}, V. A. Schegelsky¹²³, D. Scheirich¹²⁹, M. Schernau¹⁶², C. Schiavi^{52a,52b}, S. Schier¹³⁷, C. Schillo⁵⁰, M. Schioppa^{39a,39b}, S. Schlenker³², K. R. Schmidt-Sommerfeld¹⁰¹, K. Schmieden³², C. Schmitt⁸⁴, S. Schmitt⁴⁴, S. Schmitz⁸⁴, B. Schneider^{159a}, U. Schnoor⁵⁰, L. Schoeffel¹³⁶, A. Schoening^{59b}, B. D. Schoenrock⁹¹, E. Schopf²³, M. Schott⁸⁴, J. Schovancova⁸, S. Schramm⁵¹, M. Schreyer¹⁷³, N. Schuh⁸⁴, A. Schulte⁸⁴, M. J. Schultens²³, H.-C. Schultz-Coulon^{59a}, H. Schulz¹⁷, M. Schumacher⁵⁰, B. A. Schumm¹³⁷, Ph. Schune¹³⁶, A. Schwartzman¹⁴³, T. A. Schwarz⁹⁰, H. Schweiger⁸⁵, Ph. Schwemling¹³⁶, R. Schwenhorst⁹¹, J. Schwindling¹³⁶, T. Schwindt²³, G. Sciolla²⁵, F. Scuri^{124a,124b}, F. Scutti⁸⁹, J. Searcy⁹⁰, P. Seema²³, S. C. Seidel¹⁰⁵, A. Seiden¹³⁷, F. Seifert¹²⁸, J. M. Seixas^{26a}, G. Sekhniaidze^{104a}, K. Sekhon⁹⁰, S. J. Sekula⁴², D. M. Seliverstov^{123,*}, N. Semprini-Cesari^{22a,22b}, C. Serfon¹¹⁹, L. Serin¹¹⁷, L. Serkin^{163a,163b}, M. Sessa^{134a,134b}, R. Seuster¹⁶⁸, H. Severini¹¹³, T. Sfiligoi⁷⁶, F. Sforza³², A. Sfyrila⁵¹, E. Shabalina⁵⁶, N. W. Shaikh^{146a,146b}, L. Y. Shan^{35a}, R. Shang¹⁶⁵, J. T. Shank²⁴, M. Shapiro¹⁶, P. B. Shatalov⁹⁷, K. Shaw^{163a,163b}, S. M. Shaw⁸⁵, A. Shcherbakova^{146a,146b}, C. Y. Shehu¹⁴⁹, P. Sherwood⁷⁹, L. Shi^{151.ak}, S. Shimizu⁶⁸, C. O. Shimmin¹⁶², M. Shimojima¹⁰², M. Shiyakova^{66.al}, A. Shmeleva⁹⁶, D. Shoaleh Saadi⁹⁵, M. J. Shochet³³, S. Shojai^{92a,92b}, S. Shrestha¹¹¹, E. Shulga⁹⁸, M. A. Shupe⁷, P. Sicho¹²⁷, A. M. Sickles¹⁶⁵, P. E. Sidebo¹⁴⁷, O. Sidiropoulou¹⁷³, D. Sidorov¹¹⁴, A. Sidoti^{22a,22b}, F. Siegert⁴⁶, Dj. Sijacki¹⁴, J. Silva^{126a,126d}, S. B. Silverstein^{146a}, V. Simak¹²⁸, Lj. Simic¹⁴, S. Simion¹¹⁷, E. Simioni⁸⁴, B. Simmons⁷⁹, D. Simon³⁶, M. Simon⁸⁴, P. Sinervo¹⁵⁸, N. B. Sinev¹¹⁶, M. Sioli^{22a,22b}, G. Siragusa¹⁷³, S. Yu. Sivoklov⁹⁹, J. Sjölin^{146a,146b}, M. B. Skinner⁷³, H. P. Skottowe⁵⁸, P. Skubic¹¹³, M. Slater¹⁹, T. Slavicek¹²⁸, M. Slawinska¹⁰⁷, K. Sliwa¹⁶¹, R. Slovak¹²⁹, V. Smakhtin¹⁷¹, B. H. Smart⁵, L. Smestad¹⁵, J. Smiesko^{144a}, S. Yu. Smirnov⁹⁸, Y. Smirnov⁹⁸, L. N. Smirnova^{99.am}, O. Smirnova⁸², M. N. K. Smith³⁷, R. W. Smith³⁷, M. Smizanska⁷³, K. Smolek¹²⁸, A. A. Snesarev⁹⁶, S. Snyder²⁷, R. Sobie^{168.l}, F. Socher⁴⁶, A. Soffer¹⁵³, D. A. Soh¹⁵¹, G. Sokhrannyi⁷⁶, C. A. Solans Sanchez³², M. Solar¹²⁸, E. Yu. Soldatov⁹⁸, U. Soldevila¹⁶⁶, A. A. Solodkov¹³⁰, A. Soloshenko⁶⁶, O. V. Solovyanov¹³⁰, V. Solovyev¹²³, P. Sommer⁵⁰, H. Son¹⁶¹, H. Y. Song^{35b.an}, A. Sood¹⁶, A. Sopczak¹²⁸, V. Sopko¹²⁸, V. Sorin¹³, D. Sosa^{59b}, C. L. Sotiropoulou^{124a,124b}, R. Soualah^{163a,163c}, A. M. Soukharev^{109.c}, D. South⁴⁴, B. C. Sowden⁷⁸, S. Spagnolo^{74a,74b}, M. Spalla^{124a,124b}, M. Spangenberg¹⁶⁹, F. Spanò⁷⁸, D. Sperlich¹⁷, F. Spettel¹⁰¹, R. Spighi^{22a}, G. Spigo³², L. A. Spiller⁸⁹, M. Spousta¹²⁹, R. D. St. Denis^{55.*}, A. Stabile^{92a}, R. Stamen^{59a}, S. Stamm¹⁷, E. Stanecka⁴¹, R. W. Stanek⁶, C. Stanescu^{134a}, M. Stanescu-Bellu⁴⁴, M. M. Stanitzki⁴⁴, S. Stapnes¹¹⁹, E. A. Starchenko¹³⁰, G. H. Stark³³, J. Stark⁵⁷, P. Staroba¹²⁷, P. Starovoitov^{59a}, S. Stärz³², R. Staszewski⁴¹, P. Steinberg²⁷, B. Stelzer¹⁴², H. J. Stelzer³², O. Stelzer-Chilton^{159a}, H. Stenzel⁵⁴, G. A. Stewart⁵⁵, J. A. Stillings²³, M. C. Stockton⁸⁸, M. Stoebe⁸⁸, G. Stoicea^{28b}, P. Stolte⁵⁶, S. Stonjek¹⁰¹, A. R. Stradling⁸, A. Straessner⁴⁶, M. E. Stramaglia¹⁸, J. Strandberg¹⁴⁷, S. Strandberg^{146a,146b}, A. Strandlie¹¹⁹, M. Strauss¹¹³, P. Strizenec^{144b}, R. Ströhmer¹⁷³, D. M. Strom¹¹⁶, R. Stroynowski⁴², A. Strubig¹⁰⁶, S. A. Stucci²⁷, B. Stugu¹⁵, N. A. Styles⁴⁴, D. Su¹⁴³, J. Su¹²⁵, S. Suchek^{59a}, Y. Sugaya¹¹⁸, M. Suk¹²⁸, V. V. Sulin⁹⁶, S. Sultansoy^{4c}, T. Sumida⁶⁹, S. Sun⁵⁸, X. Sun^{35a}, J. E. Sundermann⁵⁰, K. Suruliz¹⁴⁹, G. Susinno^{39a,39b}, M. R. Sutton¹⁴⁹, S. Suzuki⁶⁷, M. Svatos¹²⁷, M. Swiatkowski³³, I. Sykora^{144a}, T. Sykora¹²⁹, D. Ta⁵⁰, C. Taccini^{134a,134b}, K. Tackmann⁴⁴, J. Taenzer¹⁵⁸, A. Taffard¹⁶², R. Tahirout^{159a}, N. Taiblum¹⁵³, H. Takai²⁷, R. Takashima⁷⁰, T. Takeshita¹⁴⁰, Y. Takubo⁶⁷, M. Talby⁸⁶, A. A. Talyshev^{109.c}, K. G. Tan⁸⁹, J. Tanaka¹⁵⁵, M. Tanaka¹⁵⁷, R. Tanaka¹¹⁷, S. Tanaka⁶⁷, B. B. Tannenwald¹¹¹, S. Tapia Araya^{34b}, S. Tapprogge⁸⁴, S. Tarem¹⁵², G. F. Tartarelli^{92a}, P. Tas¹²⁹, M. Tasevsky¹²⁷, T. Tashiro⁶⁹, E. Tassi^{39a,39b}, A. Tavares Delgado^{126a,126b}, Y. Tayalati^{135e}, A. C. Taylor¹⁰⁵, G. N. Taylor⁸⁹, P. T. E. Taylor⁸⁹, W. Taylor^{159b}, F. A. Teischinger³², P. Teixeira-Dias⁷⁸, K. K. Temming⁵⁰, D. Temple¹⁴², H. Ten Kate³², P. K. Teng¹⁵¹, J. J. Teoh¹¹⁸, F. Tepel¹⁷⁴, S. Terada⁶⁷, K. Terashi¹⁵⁵, J. Terron⁸³, S. Terzo¹³, M. Testa⁴⁹, R. J. Teuscher^{158.l}, T. Theveniaux-Pelzer⁸⁶, J. P. Thomas¹⁹, J. Thomas-Wilsker⁷⁸, E. N. Thompson³⁷, P. D. Thompson¹⁹, A. S. Thompson⁵⁵, L. A. Thomsen¹⁷⁵, E. Thomson¹²², M. Thomson³⁰, M. J. Tibbetts¹⁶, R. E. Ticse Torres⁸⁶, V. O. Tikhomirov^{96.ao}, Yu. A. Tikhonov^{109.c}, S. Timoshenko⁹⁸, P. Tipton¹⁷⁵, S. Tisserant⁸⁶, K. Todome¹⁵⁷, T. Todorov^{5.*}, S. Todorova-Nova¹²⁹, J. Tojo⁷¹, S. Tokár^{144a}, K. Tokushuku⁶⁷, E. Tolley⁵⁸, L. Tomlinson⁸⁵, M. Tomoto¹⁰³, L. Tompkins^{143.ap}, K. Toms¹⁰⁵, B. Tong⁵⁸, E. Torrence¹¹⁶, H. Torres¹⁴², E. Torró Pastor¹³⁸, J. Toth^{86.aq}, F. Touchard⁸⁶, D. R. Tovey¹³⁹, T. Trefzger¹⁷³, A. Tricoli²⁷, I. M. Trigger^{159a}, S. Trincaz-Duvoid⁸¹, M. F. Tripiana¹³, W. Trischuk¹⁵⁸, B. Trocmé⁵⁷, A. Trofymov⁴⁴, C. Troncon^{92a}, M. Trottier-McDonald¹⁶, M. Trovatelli¹⁶⁸, L. Truong^{163a,163c}, M. Trzebinski⁴¹, A. Trzupek⁴¹, J. C.-L. Tseng¹²⁰, P. V. Tsiarshka⁹³, G. Tsipolitis¹⁰, N. Tsirintanis⁹, S. Tsiskaridze¹³, V. Tsiskaridze⁵⁰, E. G. Tskhadadze^{53a}, K. M. Tsui^{61a}, I. I. Tsukerman⁹⁷, V. Tsulaia¹⁶, S. Tsuno⁶⁷, D. Tsybychev¹⁴⁸, Y. Tu^{61b}, A. Tudorache^{28b}, V. Tudorache^{28b}, A. N. Tuna⁵⁸, S. A. Tupper^{22a,22b}, S. Turchikhin⁶⁶, D. Turecek¹²⁸, D. Turgeman¹⁷¹, R. Turra^{92a,92b}, A. J. Turvey⁴², P. M. Tuts³⁷, M. Tyndel¹³¹, G. Ucchielli^{22a,22b}, I. Ueda¹⁵⁵, M. Ughetto^{146a,146b}, F. Ukegawa¹⁶⁰, G. Unal³², A. Undrus²⁷, G. Unel¹⁶², F. C. Ungaro⁸⁹, Y. Unno⁶⁷, C. Unverdorben¹⁰⁰, J. Urban^{144b}, P. Urquijo⁸⁹, P. Urrejola⁸⁴, G. Usai⁸, A. Usanova⁶³, L. Vacavant⁸⁶, V. Vacek¹²⁸, B. Vachon⁸⁸, C. Valderanis¹⁰⁰, E. Valdes Santurio^{146a,146b}, N. Valencic¹⁰⁷, S. Valentinetti^{22a,22b}, A. Valero¹⁶⁶, L. Valery¹³, S. Valkar¹²⁹, J. A. Valls Ferrer¹⁶⁶, W. Van Den Wollenberg¹⁰⁷, P. C. Van Der Deijl¹⁰⁷,

H. van der Graaf¹⁰⁷, N. van Eldik¹⁵², P. van Gemmeren⁶, J. Van Nieuwkoop¹⁴², I. van Vulpen¹⁰⁷, M. C. van Woerden³², M. Vanadia^{132a,132b}, W. Vandelli³², R. Vanguri¹²², A. Vaniachine¹³⁰, P. Vankov¹⁰⁷, G. Vardanyan¹⁷⁶, R. Vari^{132a}, E. W. Varnes⁷, T. Varol⁴², D. Varouchas⁸¹, A. Vartapetian⁸, K. E. Varvell¹⁵⁰, J. G. Vasquez¹⁷⁵, F. Vazeille³⁶, T. Vazquez Schroeder⁸⁸, J. Veatch⁵⁶, V. Veeraraghavan⁷, L. M. Veloce¹⁵⁸, F. Veloso^{126a,126c}, S. Veneziano^{132a}, A. Ventura^{74a,74b}, M. Venturi¹⁶⁸, N. Venturi¹⁵⁸, A. Venturini²⁵, V. Vercesi^{121a}, M. Verducci^{132a,132b}, W. Verkerke¹⁰⁷, J. C. Vermeulen¹⁰⁷, A. Vest^{46,ar}, M. C. Vetterli^{142,d}, O. Viazlo⁸², I. Vichou^{165,*}, T. Vickey¹³⁹, O. E. Vickey Boeriu¹³⁹, G. H. A. Viehhauser¹²⁰, S. Viel¹⁶, L. Vigani¹²⁰, M. Villa^{22a,22b}, M. Villaplana Perez^{92a,92b}, E. Vilucchi⁴⁹, M. G. Vinciter³¹, V. B. Vinogradov⁶⁶, C. Vittori^{22a,22b}, I. Vivarelli¹⁴⁹, S. Vlachos¹⁰, M. Vlasak¹²⁸, M. Vogel¹⁷⁴, P. Vokac¹²⁸, G. Volpi^{124a,124b}, M. Volpi⁸⁹, H. von der Schmitt¹⁰¹, E. von Toerne²³, V. Vorobel¹²⁹, K. Vorobev⁹⁸, M. Vos¹⁶⁶, R. Voss³², J. H. Vossebeld⁷⁵, N. Vranjes¹⁴, M. Vranjes Milosavljevic¹⁴, V. Vrba¹²⁷, M. Vreeswijk¹⁰⁷, R. Vuillermet³², I. Vukotic³³, Z. Vykydal¹²⁸, P. Wagner²³, W. Wagner¹⁷⁴, H. Wahlberg⁷², S. Wahrmund⁴⁶, J. Wakabayashi¹⁰³, J. Walder⁷³, R. Walker¹⁰⁰, W. Walkowiak¹⁴¹, V. Wallangen^{146a,146b}, C. Wang^{35c}, C. Wang^{35d,86}, F. Wang¹⁷², H. Wang¹⁶, H. Wang⁴², J. Wang⁴⁴, J. Wang¹⁵⁰, K. Wang⁸⁸, R. Wang⁶, S. M. Wang¹⁵¹, T. Wang²³, T. Wang³⁷, W. Wang^{35b}, X. Wang¹⁷⁵, C. Wanotayaroj¹¹⁶, A. Warburton⁸⁸, C. P. Ward³⁰, D. R. Wardrope⁷⁹, A. Washbrook⁴⁸, P. M. Watkins¹⁹, A. T. Watson¹⁹, M. F. Watson¹⁹, G. Watts¹³⁸, S. Watts⁸⁵, B. M. Waugh⁷⁹, S. Webb⁸⁴, M. S. Weber¹⁸, S. W. Weber¹⁷³, J. S. Webster⁶, A. R. Weidberg¹²⁰, B. Weinert⁶², J. Weingarten⁵⁶, C. Weiser⁵⁰, H. Weits¹⁰⁷, P. S. Wells³², T. Wenaus²⁷, T. Wengler³², S. Wenig³², N. Wermes²³, M. Werner⁵⁰, M. D. Werner⁶⁵, P. Werner³², M. Wessels^{59a}, J. Wetter¹⁶¹, K. Whalen¹¹⁶, N. L. Whallon¹³⁸, A. M. Wharton⁷³, A. White⁸, M. J. White¹, R. White^{34b}, D. Whiteson¹⁶², F. J. Wickens¹³¹, W. Wiedenmann¹⁷², M. WIELERS¹³¹, P. Wienemann²³, C. Wiglesworth³⁸, L. A. M. Wiik-Fuchs²³, A. Wildauer¹⁰¹, F. Wilk⁸⁵, H. G. Wilkens³², H. H. Williams¹²², S. Williams¹⁰⁷, C. Willis⁹¹, S. Willocq⁸⁷, J. A. Wilson¹⁹, I. Wingerter-Seez⁵, F. Winklmeier¹¹⁶, O. J. Winston¹⁴⁹, B. T. Winter²³, M. Wittgen¹⁴³, J. Wittkowski¹⁰⁰, T. M. H. Wolf¹⁰⁷, M. W. Wolter⁴¹, H. Wolters^{126a,126c}, S. D. Worm¹³¹, B. K. Wosiek⁴¹, J. Wotschack³², M. J. Woudstra⁸⁵, K. W. Wozniak⁴¹, M. Wu⁵⁷, M. Wu³³, S. L. Wu¹⁷², X. Wu⁵¹, Y. Wu⁹⁰, T. R. Wyatt⁸⁵, B. M. Wynne⁴⁸, S. Xella³⁸, D. Xu^{35a}, L. Xu²⁷, B. Yabsley¹⁵⁰, S. Yacoub^{145a}, D. Yamaguchi¹⁵⁷, Y. Yamaguchi¹¹⁸, A. Yamamoto⁶⁷, S. Yamamoto¹⁵⁵, T. Yamanaka¹⁵⁵, K. Yamauchi¹⁰³, Y. Yamazaki⁶⁸, Z. Yan²⁴, H. Yang^{35e}, H. Yang¹⁷², Y. Yang¹⁵¹, Z. Yang¹⁵, W.-M. Yao¹⁶, Y. C. Yap⁸¹, Y. Yasu⁶⁷, E. Yatsenko⁵, K. H. Yau Wong²³, J. Ye⁴², S. Ye²⁷, I. Yeletsikh⁶⁶, A. L. Yen⁵⁸, E. Yildirim⁸⁴, K. Yoritani¹⁷⁰, R. Yoshida⁶, K. Yoshihara¹²², C. Young¹⁴³, C. J. S. Young³², S. Youssef²⁴, D. R. Yu¹⁶, J. Yu⁸, J. M. Yu⁹⁰, J. Yu⁶⁵, L. Yuan⁶⁸, S. P. Y. Yuen²³, I. Yusuff^{30,as}, B. Zabinski⁴¹, R. Zaidan^{35d}, A. M. Zaitsev^{130,ae}, N. Zakharchuk⁴⁴, J. Zalieckas¹⁵, A. Zaman¹⁴⁸, S. Zambito⁵⁸, L. Zanello^{132a,132b}, D. Zanzi⁸⁹, C. Zeitnitz¹⁷⁴, M. Zeman¹²⁸, A. Zemla^{40a}, J. C. Zeng¹⁶⁵, Q. Zeng¹⁴³, K. Zengel²⁵, O. Zenin¹³⁰, T. Ženiš^{144a}, D. Zerwas¹¹⁷, D. Zhang⁹⁰, F. Zhang¹⁷², G. Zhang^{35b,an}, H. Zhang^{35c}, J. Zhang⁶, L. Zhang⁵⁰, R. Zhang²³, R. Zhang^{35b,at}, X. Zhang^{35d}, Z. Zhang¹¹⁷, X. Zhao⁴², Y. Zhao^{35d}, Z. Zhao^{35b}, A. Zhemchugov⁶⁶, J. Zhong¹²⁰, B. Zhou⁹⁰, C. Zhou⁴⁷, L. Zhou³⁷, L. Zhou⁴², M. Zhou¹⁴⁸, N. Zhou^{35f}, C. G. Zhu^{35d}, H. Zhu^{35a}, J. Zhu⁹⁰, Y. Zhu^{35b}, X. Zhuang^{35a}, K. Zhukov⁹⁶, A. Zibell¹⁷³, D. Zieminska⁶², N. I. Zimine⁶⁶, C. Zimmermann⁸⁴, S. Zimmermann⁵⁰, Z. Zinonos⁵⁶, M. Zinser⁸⁴, M. Ziolkowski¹⁴¹, L. Živković¹⁴, G. Zobernig¹⁷², A. Zoccoli^{22a,22b}, M. zur Nedden¹⁷, L. Zwalinski³²

¹ Department of Physics, University of Adelaide, Adelaide, Australia

² Physics Department, SUNY Albany, Albany, NY, USA

³ Department of Physics, University of Alberta, Edmonton, AB, Canada

⁴ (a) Department of Physics, Ankara University, Ankara, Turkey; (b) Istanbul Aydin University, Istanbul, Turkey; (c) Division of Physics, TOBB University of Economics and Technology, Ankara, Turkey

⁵ LAPP, CNRS/IN2P3 and Université Savoie Mont Blanc, Annecy-le-Vieux, France

⁶ High Energy Physics Division, Argonne National Laboratory, Argonne, IL, USA

⁷ Department of Physics, University of Arizona, Tucson, AZ, USA

⁸ Department of Physics, The University of Texas at Arlington, Arlington, TX, USA

⁹ Physics Department, University of Athens, Athens, Greece

¹⁰ Physics Department, National Technical University of Athens, Zografou, Greece

¹¹ Department of Physics, The University of Texas at Austin, Austin, TX, USA

¹² Institute of Physics, Azerbaijan Academy of Sciences, Baku, Azerbaijan

¹³ Institut de Física d'Altes Energies (IFAE), The Barcelona Institute of Science and Technology, Barcelona, Spain

¹⁴ Institute of Physics, University of Belgrade, Belgrade, Serbia

¹⁵ Department for Physics and Technology, University of Bergen, Bergen, Norway

¹⁶ Physics Division, Lawrence Berkeley National Laboratory and University of California, Berkeley, CA, USA

¹⁷ Department of Physics, Humboldt University, Berlin, Germany

- ¹⁸ Albert Einstein Center for Fundamental Physics and Laboratory for High Energy Physics, University of Bern, Bern, Switzerland
- ¹⁹ School of Physics and Astronomy, University of Birmingham, Birmingham, UK
- ²⁰ (a) Department of Physics, Bogazici University, Istanbul, Turkey; (b) Department of Physics Engineering, Gaziantep University, Gaziantep, Turkey; (c) Faculty of Engineering and Natural Sciences, Istanbul Bilgi University, Istanbul, Turkey; (d) Faculty of Engineering and Natural Sciences, Bahcesehir University, Istanbul, Turkey
- ²¹ Centro de Investigaciones, Universidad Antonio Narino, Bogotá, Colombia
- ²² (a) INFN Sezione di Bologna, Bologna, Italy; (b) Dipartimento di Fisica e Astronomia, Università di Bologna, Bologna, Italy
- ²³ Physikalisches Institut, University of Bonn, Bonn, Germany
- ²⁴ Department of Physics, Boston University, Boston, MA, USA
- ²⁵ Department of Physics, Brandeis University, Waltham, MA, USA
- ²⁶ (a) Universidade Federal do Rio De Janeiro COPPE/EE/IF, Rio de Janeiro, Brazil; (b) Electrical Circuits Department, Federal University of Juiz de Fora (UFJF), Juiz de Fora, Brazil; (c) Federal University of Sao Joao del Rei (UFSJ), Sao Joao del Rei, Brazil; (d) Instituto de Fisica, Universidade de Sao Paulo, São Paulo, Brazil
- ²⁷ Physics Department, Brookhaven National Laboratory, Upton, NY, USA
- ²⁸ (a) Transilvania University of Brasov, Brasov, Romania; (b) National Institute of Physics and Nuclear Engineering, Bucharest, Romania; (c) Physics Department, National Institute for Research and Development of Isotopic and Molecular Technologies, Cluj Napoca, Romania; (d) University Politehnica Bucharest, Bucharest, Romania; (e) West University in Timisoara, Timisoara, Romania
- ²⁹ Departamento de Física, Universidad de Buenos Aires, Buenos Aires, Argentina
- ³⁰ Cavendish Laboratory, University of Cambridge, Cambridge, UK
- ³¹ Department of Physics, Carleton University, Ottawa, ON, Canada
- ³² CERN, Geneva, Switzerland
- ³³ Enrico Fermi Institute, University of Chicago, Chicago, IL, USA
- ³⁴ (a) Departamento de Física, Pontificia Universidad Católica de Chile, Santiago, Chile; (b) Departamento de Física, Universidad Técnica Federico Santa María, Valparaiso, Chile
- ³⁵ (a) Institute of High Energy Physics, Chinese Academy of Sciences, Beijing, China; (b) Department of Modern Physics, University of Science and Technology of China, Hefei, Anhui, China; (c) Department of Physics, Nanjing University, Nanjing, Jiangsu, China; (d) School of Physics, Shandong University, Jinan, Shandong, China; (e) Shanghai Key Laboratory for Particle Physics and Cosmology, Department of Physics and Astronomy, Shanghai Jiao Tong University (also affiliated with PKU-CHEP), Shanghai, China; (f) Physics Department, Tsinghua University, Beijing 100084, China
- ³⁶ Laboratoire de Physique Corpusculaire, Clermont Université and Université Blaise Pascal and CNRS/IN2P3, Clermont-Ferrand, France
- ³⁷ Nevis Laboratory, Columbia University, Irvington, NY, USA
- ³⁸ Niels Bohr Institute, University of Copenhagen, Copenhagen, Denmark
- ³⁹ (a) INFN Gruppo Collegato di Cosenza, Laboratori Nazionali di Frascati, Frascati, Italy; (b) Dipartimento di Fisica, Università della Calabria, Rende, Italy
- ⁴⁰ (a) Faculty of Physics and Applied Computer Science, AGH University of Science and Technology, Kraków, Poland; (b) Marian Smoluchowski Institute of Physics, Jagiellonian University, Kraków, Poland
- ⁴¹ Institute of Nuclear Physics, Polish Academy of Sciences, Kraków, Poland
- ⁴² Physics Department, Southern Methodist University, Dallas, TX, USA
- ⁴³ Physics Department, University of Texas at Dallas, Richardson, TX, USA
- ⁴⁴ DESY, Hamburg, Zeuthen, Germany
- ⁴⁵ Lehrstuhl für Experimentelle Physik IV, Technische Universität Dortmund, Dortmund, Germany
- ⁴⁶ Institut für Kern- und Teilchenphysik, Technische Universität Dresden, Dresden, Germany
- ⁴⁷ Department of Physics, Duke University, Durham, NC, USA
- ⁴⁸ SUPA-School of Physics and Astronomy, University of Edinburgh, Edinburgh, UK
- ⁴⁹ INFN Laboratori Nazionali di Frascati, Frascati, Italy
- ⁵⁰ Fakultät für Mathematik und Physik, Albert-Ludwigs-Universität, Freiburg, Germany
- ⁵¹ Section de Physique, Université de Genève, Geneva, Switzerland
- ⁵² (a) INFN Sezione di Genova, Genoa, Italy; (b) Dipartimento di Fisica, Università di Genova, Genoa, Italy

- 53 (a)E. Andronikashvili Institute of Physics, Iv. Javakhishvili Tbilisi State University, Tbilisi, Georgia; (b)High Energy Physics Institute, Tbilisi State University, Tbilisi, Georgia
- 54 II Physikalisches Institut, Justus-Liebig-Universität Giessen, Giessen, Germany
- 55 SUPA-School of Physics and Astronomy, University of Glasgow, Glasgow, UK
- 56 II Physikalisches Institut, Georg-August-Universität, Göttingen, Germany
- 57 Laboratoire de Physique Subatomique et de Cosmologie, Université Grenoble-Alpes, CNRS/IN2P3, Grenoble, France
- 58 Laboratory for Particle Physics and Cosmology, Harvard University, Cambridge, MA, USA
- 59 (a)Kirchhoff-Institut für Physik, Ruprecht-Karls-Universität Heidelberg, Heidelberg, Germany; (b)Physikalisches Institut, Ruprecht-Karls-Universität Heidelberg, Heidelberg, Germany; (c)ZITI Institut für technische Informatik, Ruprecht-Karls-Universität Heidelberg, Mannheim, Germany
- 60 Faculty of Applied Information Science, Hiroshima Institute of Technology, Hiroshima, Japan
- 61 (a)Department of Physics, The Chinese University of Hong Kong, Shatin, N.T., Hong Kong; (b)Department of Physics, The University of Hong Kong, Pok Fu Lam, Hong Kong; (c)Department of Physics, The Hong Kong University of Science and Technology, Clear Water Bay, Kowloon, Hong Kong, China
- 62 Department of Physics, Indiana University, Bloomington, IN, USA
- 63 Institut für Astro- und Teilchenphysik, Leopold-Franzens-Universität, Innsbruck, Austria
- 64 University of Iowa, Iowa City, IA, USA
- 65 Department of Physics and Astronomy, Iowa State University, Ames, IA, USA
- 66 Joint Institute for Nuclear Research, JINR Dubna, Dubna, Russia
- 67 KEK, High Energy Accelerator Research Organization, Tsukuba, Japan
- 68 Graduate School of Science, Kobe University, Kobe, Japan
- 69 Faculty of Science, Kyoto University, Kyoto, Japan
- 70 Kyoto University of Education, Kyoto, Japan
- 71 Department of Physics, Kyushu University, Fukuoka, Japan
- 72 Instituto de Física La Plata, Universidad Nacional de La Plata and CONICET, La Plata, Argentina
- 73 Physics Department, Lancaster University, Lancaster, UK
- 74 (a)INFN Sezione di Lecce, Lecce, Italy; (b)Dipartimento di Matematica e Fisica, Università del Salento, Lecce, Italy
- 75 Oliver Lodge Laboratory, University of Liverpool, Liverpool, UK
- 76 Department of Physics, Jožef Stefan Institute and University of Ljubljana, Ljubljana, Slovenia
- 77 School of Physics and Astronomy, Queen Mary University of London, London, UK
- 78 Department of Physics, Royal Holloway University of London, Surrey, UK
- 79 Department of Physics and Astronomy, University College London, London, UK
- 80 Louisiana Tech University, Ruston, LA, USA
- 81 Laboratoire de Physique Nucléaire et de Hautes Energies, UPMC and Université Paris-Diderot and CNRS/IN2P3, Paris, France
- 82 Fysiska Institutionen, Lunds Universitet, Lund, Sweden
- 83 Departamento de Física Teórica C-15, Universidad Autónoma de Madrid, Madrid, Spain
- 84 Institut für Physik, Universität Mainz, Mainz, Germany
- 85 School of Physics and Astronomy, University of Manchester, Manchester, UK
- 86 CPPM, Aix-Marseille Université and CNRS/IN2P3, Marseille, France
- 87 Department of Physics, University of Massachusetts, Amherst, MA, USA
- 88 Department of Physics, McGill University, Montreal, QC, Canada
- 89 School of Physics, University of Melbourne, Melbourne, VIC, Australia
- 90 Department of Physics, The University of Michigan, Ann Arbor, MI, USA
- 91 Department of Physics and Astronomy, Michigan State University, East Lansing, MI, USA
- 92 (a)INFN Sezione di Milano, Milan, Italy; (b)Dipartimento di Fisica, Università di Milano, Milan, Italy
- 93 B.I. Stepanov Institute of Physics, National Academy of Sciences of Belarus, Minsk, Republic of Belarus
- 94 National Scientific and Educational Centre for Particle and High Energy Physics, Minsk, Republic of Belarus
- 95 Group of Particle Physics, University of Montreal, Montreal, QC, Canada
- 96 P.N. Lebedev Physical Institute of the Russian Academy of Sciences, Moscow, Russia
- 97 Institute for Theoretical and Experimental Physics (ITEP), Moscow, Russia
- 98 National Research Nuclear University MEPhI, Moscow, Russia
- 99 D.V. Skobeltsyn Institute of Nuclear Physics, M.V. Lomonosov Moscow State University, Moscow, Russia

- 100 Fakultät für Physik, Ludwig-Maximilians-Universität München, Munich, Germany
- 101 Max-Planck-Institut für Physik (Werner-Heisenberg-Institut), Munich, Germany
- 102 Nagasaki Institute of Applied Science, Nagasaki, Japan
- 103 Graduate School of Science and Kobayashi-Maskawa Institute, Nagoya University, Nagoya, Japan
- 104 ^(a)INFN Sezione di Napoli, Naples, Italy; ^(b)Dipartimento di Fisica, Università di Napoli, Naples, Italy
- 105 Department of Physics and Astronomy, University of New Mexico, Albuquerque, NM, USA
- 106 Institute for Mathematics, Astrophysics and Particle Physics, Radboud University Nijmegen/Nikhef, Nijmegen, The Netherlands
- 107 Nikhef National Institute for Subatomic Physics and University of Amsterdam, Amsterdam, The Netherlands
- 108 Department of Physics, Northern Illinois University, DeKalb, IL, USA
- 109 Budker Institute of Nuclear Physics, SB RAS, Novosibirsk, Russia
- 110 Department of Physics, New York University, New York, NY, USA
- 111 Ohio State University, Columbus, OH, USA
- 112 Faculty of Science, Okayama University, Okayama, Japan
- 113 Homer L. Dodge Department of Physics and Astronomy, University of Oklahoma, Norman, OK, USA
- 114 Department of Physics, Oklahoma State University, Stillwater, OK, USA
- 115 Palacký University, RCPTM, Olomouc, Czech Republic
- 116 Center for High Energy Physics, University of Oregon, Eugene, OR, USA
- 117 LAL, University of Paris-Sud, CNRS/IN2P3, Université Paris-Saclay, Orsay, France
- 118 Graduate School of Science, Osaka University, Osaka, Japan
- 119 Department of Physics, University of Oslo, Oslo, Norway
- 120 Department of Physics, Oxford University, Oxford, UK
- 121 ^(a)INFN Sezione di Pavia, Pavia, Italy; ^(b)Dipartimento di Fisica, Università di Pavia, Pavia, Italy
- 122 Department of Physics, University of Pennsylvania, Philadelphia, PA, USA
- 123 National Research Centre “Kurchatov Institute” B.P. Konstantinov Petersburg Nuclear Physics Institute, St. Petersburg, Russia
- 124 ^(a)INFN Sezione di Pisa, Pisa, Italy; ^(b)Dipartimento di Fisica E. Fermi, Università di Pisa, Pisa, Italy
- 125 Department of Physics and Astronomy, University of Pittsburgh, Pittsburgh, PA, USA
- 126 ^(a)Laboratório de Instrumentação e Física Experimental de Partículas-LIP, Lisbon, Portugal; ^(b)Faculdade de Ciências, Universidade de Lisboa, Lisbon, Portugal; ^(c)Department of Physics, University of Coimbra, Coimbra, Portugal; ^(d)Centro de Física Nuclear da Universidade de Lisboa, Lisbon, Portugal; ^(e)Departamento de Física, Universidade do Minho, Braga, Portugal; ^(f)Departamento de Física Teórica y del Cosmos and CAFPE, Universidad de Granada, Granada, Spain; ^(g)Dep Física and CEFITEC of Faculdade de Ciências e Tecnologia, Universidade Nova de Lisboa, Caparica, Portugal
- 127 Institute of Physics, Academy of Sciences of the Czech Republic, Prague, Czech Republic
- 128 Czech Technical University in Prague, Prague, Czech Republic
- 129 Faculty of Mathematics and Physics, Charles University in Prague, Prague, Czech Republic
- 130 State Research Center Institute for High Energy Physics (Protvino), NRC KI, Protvino, Russia
- 131 Particle Physics Department, Rutherford Appleton Laboratory, Didcot, UK
- 132 ^(a)INFN Sezione di Roma, Rome, Italy; ^(b)Dipartimento di Fisica, Sapienza Università di Roma, Rome, Italy
- 133 ^(a)INFN Sezione di Roma Tor Vergata, Rome, Italy; ^(b)Dipartimento di Fisica, Università di Roma Tor Vergata, Rome, Italy
- 134 ^(a)INFN Sezione di Roma Tre, Rome, Italy; ^(b)Dipartimento di Matematica e Fisica, Università Roma Tre, Rome, Italy
- 135 ^(a)Faculté des Sciences Ain Chock, Réseau Universitaire de Physique des Hautes Energies-Université Hassan II, Casablanca, Morocco; ^(b)Centre National de l’Energie des Sciences Techniques Nucleaires, Rabat, Morocco; ^(c)Faculté des Sciences Semlalia, Université Cadi Ayyad, LPHEA-Marrakech, Marrakech, Morocco; ^(d)Faculté des Sciences, Université Mohamed Premier and LTPM, Oujda, Morocco; ^(e)Faculté des Sciences, Université Mohammed V, Rabat, Morocco
- 136 DSM/IRFU (Institut de Recherches sur les Lois Fondamentales de l’Univers), CEA Saclay (Commissariat à l’Energie Atomique et aux Energies Alternatives), Gif-sur-Yvette, France
- 137 Santa Cruz Institute for Particle Physics, University of California Santa Cruz, Santa Cruz, CA, USA
- 138 Department of Physics, University of Washington, Seattle, WA, USA
- 139 Department of Physics and Astronomy, University of Sheffield, Sheffield, UK

- 140 Department of Physics, Shinshu University, Nagano, Japan
 - 141 Fachbereich Physik, Universität Siegen, Siegen, Germany
 - 142 Department of Physics, Simon Fraser University, Burnaby, BC, Canada
 - 143 SLAC National Accelerator Laboratory, Stanford, CA, USA
 - 144 (a) Faculty of Mathematics, Physics and Informatics, Comenius University, Bratislava, Slovak Republic; (b) Department of Subnuclear Physics, Institute of Experimental Physics of the Slovak Academy of Sciences, Kosice, Slovak Republic
 - 145 (a) Department of Physics, University of Cape Town, Cape Town, South Africa; (b) Department of Physics, University of Johannesburg, Johannesburg, South Africa; (c) School of Physics, University of the Witwatersrand, Johannesburg, South Africa
 - 146 (a) Department of Physics, Stockholm University, Stockholm, Sweden; (b) The Oskar Klein Centre, Stockholm, Sweden
 - 147 Physics Department, Royal Institute of Technology, Stockholm, Sweden
 - 148 Departments of Physics and Astronomy and Chemistry, Stony Brook University, Stony Brook, NY, USA
 - 149 Department of Physics and Astronomy, University of Sussex, Brighton, UK
 - 150 School of Physics, University of Sydney, Sydney, Australia
 - 151 Institute of Physics, Academia Sinica, Taipei, Taiwan
 - 152 Department of Physics, Technion: Israel Institute of Technology, Haifa, Israel
 - 153 Raymond and Beverly Sackler School of Physics and Astronomy, Tel Aviv University, Tel Aviv, Israel
 - 154 Department of Physics, Aristotle University of Thessaloniki, Thessaloniki, Greece
 - 155 International Center for Elementary Particle Physics and Department of Physics, The University of Tokyo, Tokyo, Japan
 - 156 Graduate School of Science and Technology, Tokyo Metropolitan University, Tokyo, Japan
 - 157 Department of Physics, Tokyo Institute of Technology, Tokyo, Japan
 - 158 Department of Physics, University of Toronto, Toronto, ON, Canada
 - 159 (a) TRIUMF, Vancouver, BC, Canada; (b) Department of Physics and Astronomy, York University, Toronto, ON, Canada
 - 160 Faculty of Pure and Applied Sciences, and Center for Integrated Research in Fundamental Science and Engineering, University of Tsukuba, Tsukuba, Japan
 - 161 Department of Physics and Astronomy, Tufts University, Medford, MA, USA
 - 162 Department of Physics and Astronomy, University of California Irvine, Irvine, CA, USA
 - 163 (a) INFN Gruppo Collegato di Udine, Sezione di Trieste, Udine, Italy; (b) ICTP, Trieste, Italy; (c) Dipartimento di Chimica Fisica e Ambiente, Università di Udine, Udine, Italy
 - 164 Department of Physics and Astronomy, University of Uppsala, Uppsala, Sweden
 - 165 Department of Physics, University of Illinois, Urbana, IL, USA
 - 166 Instituto de Física Corpuscular (IFIC) and Departamento de Física Atomica, Molecular y Nuclear and Departamento de Ingeniería Electrónica and Instituto de Microelectrónica de Barcelona (IMB-CNM), University of Valencia and CSIC, Valencia, Spain
 - 167 Department of Physics, University of British Columbia, Vancouver, BC, Canada
 - 168 Department of Physics and Astronomy, University of Victoria, Victoria, BC, Canada
 - 169 Department of Physics, University of Warwick, Coventry, UK
 - 170 Waseda University, Tokyo, Japan
 - 171 Department of Particle Physics, The Weizmann Institute of Science, Rehovot, Israel
 - 172 Department of Physics, University of Wisconsin, Madison, WI, USA
 - 173 Fakultät für Physik und Astronomie, Julius-Maximilians-Universität, Würzburg, Germany
 - 174 Fakultät für Mathematik und Naturwissenschaften, Fachgruppe Physik, Bergische Universität Wuppertal, Wuppertal, Germany
 - 175 Department of Physics, Yale University, New Haven, CT, USA
 - 176 Yerevan Physics Institute, Yerevan, Armenia
 - 177 Centre de Calcul de l'Institut National de Physique Nucléaire et de Physique des Particules (IN2P3), Villeurbanne, France
- ^a Also at Department of Physics, King's College London, London, UK
- ^b Also at Institute of Physics, Azerbaijan Academy of Sciences, Baku, Azerbaijan
- ^c Also at Novosibirsk State University, Novosibirsk, Russia
- ^d Also at TRIUMF, Vancouver, BC, Canada
- ^e Also at Department of Physics and Astronomy, University of Louisville, Louisville, KY, USA
- ^f Also at Department of Physics, California State University, Fresno, CA, USA

- ^g Also at Department of Physics, University of Fribourg, Fribourg, Switzerland
- ^h Also at Departament de Física de la Universitat Autònoma de Barcelona, Barcelona, Spain
- ⁱ Also at Departamento de Física e Astronomia, Faculdade de Ciências, Universidade do Porto, Porto, Portugal
- ^j Also at Tomsk State University, Tomsk, Russia
- ^k Also at Università di Napoli Parthenope, Naples, Italy
- ^l Also at Institute of Particle Physics (IPP), Victoria, BC, Canada
- ^m Also at National Institute of Physics and Nuclear Engineering, Bucharest, Romania
- ⁿ Also at Department of Physics, St. Petersburg State Polytechnical University, St. Petersburg, Russia
- ^o Also at Department of Physics, The University of Michigan, Ann Arbor, MI, USA
- ^p Also at Centre for High Performance Computing, CSIR Campus, Rosebank, Cape Town, South Africa
- ^q Also at Louisiana Tech University, Ruston, LA, USA
- ^r Also at Institutio Catalana de Recerca i Estudis Avancats, ICREA, Barcelona, Spain
- ^s Also at Graduate School of Science, Osaka University, Osaka, Japan
- ^t Also at Department of Physics, National Tsing Hua University, Hsinchu, Taiwan
- ^u Also at Institute for Mathematics, Astrophysics and Particle Physics, Radboud University Nijmegen/Nikhef, Nijmegen, The Netherlands
- ^v Also at Department of Physics, The University of Texas at Austin, Austin, TX, USA
- ^w Also at Institute of Theoretical Physics, Ilia State University, Tbilisi, Georgia
- ^x Also at CERN, Geneva, Switzerland
- ^y Also at Georgian Technical University (GTU), Tbilisi, Georgia
- ^z Also at O Chadai Academic Production, Ochanomizu University, Tokyo, Japan
- ^{aa} Also at Manhattan College, New York, NY, USA
- ^{ab} Also at Hellenic Open University, Patras, Greece
- ^{ac} Also at Academia Sinica Grid Computing, Institute of Physics, Academia Sinica, Taipei, Taiwan
- ^{ad} Also at School of Physics, Shandong University, Jinan, Shandong, China
- ^{ae} Also at Moscow Institute of Physics and Technology State University, Dolgoprudny, Russia
- ^{af} Also at Section de Physique, Université de Genève, Geneva, Switzerland
- ^{ag} Also at Eotvos Lorand University, Budapest, Hungary
- ^{ah} Also at Departments of Physics and Astronomy and Chemistry, Stony Brook University, Stony Brook, NY, USA
- ^{ai} Also at International School for Advanced Studies (SISSA), Trieste, Italy
- ^{aj} Also at Department of Physics and Astronomy, University of South Carolina, Columbia, SC, USA
- ^{ak} Also at School of Physics and Engineering, Sun Yat-sen University, Guangzhou, China
- ^{al} Also at Institute for Nuclear Research and Nuclear Energy (INRNE) of the Bulgarian Academy of Sciences, Sofia, Bulgaria
- ^{am} Also at Faculty of Physics, M.V. Lomonosov Moscow State University, Moscow, Russia
- ^{an} Also at Institute of Physics, Academia Sinica, Taipei, Taiwan
- ^{ao} Also at National Research Nuclear University MEPhI, Moscow, Russia
- ^{ap} Also at Department of Physics, Stanford University, Stanford, CA, USA
- ^{aq} Also at Institute for Particle and Nuclear Physics, Wigner Research Centre for Physics, Budapest, Hungary
- ^{ar} Also at Flensburg University of Applied Sciences, Flensburg, Germany
- ^{as} Also at University of Malaya, Department of Physics, Kuala Lumpur, Malaysia
- ^{at} Also at CPPM, Aix-Marseille Université and CNRS/IN2P3, Marseille, France
- * Deceased